REPORT

No.: D3.3 – part 4

Axially loaded sandwich panels

Publisher:	Saskia Käpplein
	Thomas Misiek
	Karlsruher Institut für Technologie (KIT)
	Versuchsanstalt für Stahl, Holz und Steine

Task:	3.4
Object:	Design of axially loaded sandwich panels, global load-bearing behaviour

This report includes 63 pages and 2 annexes.

Date of issue: 01.06.2011

Project co-funded under the European Commission Seventh Research and Technology Development Framework Programme (2007-2013)		
Theme 4 NMP-Nanotechnologies, Materials and new Production Technologies		
Prepared by		
Saskia Käpplein, Thomas Misiek, Karlsruher Institut für Technologie (KIT), Versuchsanstalt für Stahl, Holz und Steine		
Drafting History		
Draft Version 1.1	23.05.2011	
Draft Version 1.2	31.05.2011	
Draft Version 1.3		
Draft Version 1.4		
Final	01.06.2011	
Dissemination Level		
PU	Public	X
PP	Restricted to the other programme participants (including the Commission Services)	
RE	Restricted to a group specified by the Consortium (including the Commission Services)	
CO	Confidential, only for members of the Consortium (including the Commission Services)	
Verification and approval		
Coordinator		
Industrial Project Leader		
Management Committee		
Industrial Committee		
Deliverable		
D3.3 – part 4: Axially loaded sandwich panels		Due date: Month 35 Completed: Month 33

Table of contents

Symbols and notations

A_C cross section area of core

A_F cross section area of face

B width of panel

B_S bending rigidity of a sandwich panel

C_{my} equivalent uniform moment factor (equivalent member method)

D thickness of panel, for panels with flat or lightly profiled faces also distance of centroids of faces

E_F elastic modulus of face

E_C elastic modulus of core

GA shear rigidity of panel, elastic buckling load due to shear rigidity

G_C shear modulus of core

L length of panel, span of panel

M bending moment

M^N fixed end moment due to eccentric axial force

M_T moment due to temperature differences

M_w maximum bending moment of a sandwich panel

N normal force, axial load

N_{cr} elastic buckling load of a sandwich panel

N_{ki} elastic buckling load due to bending rigidity (faces)

N_w axial wrinkling force, maximum compressive axial force

P concentrated transverse load (point load)

V transverse force

e_0 initial deflection, global imperfection

f_{Cv} shear strength of core

k relationship between deflection due to shear and deflection due to bending

k_{yy} interaction factor (equivalent member method)

q linear load, distributed load

q_{e0} equivalent load (due to initial deflection and axial force)

t_F thickness of face sheet

w deflection

w_b deflection due to bending

w_T deflection due to temperature difference

w_v deflection due to transverse force

w_{st} deflection due to short-term load

w_{lt} deflection due to long-term load

α amplification factor to consider effects of 2nd Order Theory

α imperfection factor (equivalent member method)

α_F thermal expansion coefficient of the face

γ shear deformation

λ slenderness

λ_{ki} bending slenderness

λ_{GA} shear slenderness

σ_F normal stress in the face

σ_w wrinkling stress

τ_C shear stress in the core

φ_t creep coefficient

φ_{St} sandwich creep coefficient

χ reduction factor (equivalent member method)

ΔT temperature difference between inner face and outer face

M^I, V^I, w^i moment, transverse force, deflection calculated by 1st Order Theory

M^{II}, V^{II}, w^{ii} moment, transverse force, deflection calculated by 2nd Order Theory

1 Introduction

Until now the common application of sandwich panels is restricted to the function of space enclosure. The sandwich panels are mounted on a substructure and they transfer transverse loads as wind and snow to the substructure. The sandwich panels are subjected to bending moments and transverse forces only. A new application is to apply sandwich panels with flat or lightly profiled faces in smaller buildings – such as cooling chambers, climatic chambers and clean rooms – without any load transferring substructure (Fig. 1.1).

Fig. 1.1:   **Building made of sandwich panels but without substructure**

In this new type of application in addition to space enclosure, the sandwich panels have to transfer loads and to stabilise the building. In addition to the moments and transverse forces resulting from transverse loads, the wall panels transfer normal forces arising from the super-imposed load from overlying roof or ceiling panels. That implies the question about the load-bearing behaviour and the load bearing capacity of sandwich panels subjected to axial load or a combination from axial and transverse loads.

Design procedures for sandwich panels subjected to bending moments and transverse forces are given in EN 14509 [1] and in different (national) approvals. But there are no general design methods for panels subjected to axial loads or a combination of axial and transverse loads available. There are some publications, which mainly deal with the elastic buckling load of axially loaded sandwich panels, e.g. [10]. Also some mainly theoretical investigations on the interaction of elastic global buckling and elastic local buckling (wrinkling) have been done, e.g. [16], [17]. But the available investigations do not result in a design procedure, which can be used to design axially loaded sandwich panels, because these investigations basically deal with elastic buckling behaviour. Furthermore the influence of long-term loads (creep of core material) is not considered at all.

Within the framework of WP3 of the EASIE project, a design method for axially loaded sandwich panels has been developed. Buckling and long-term tests on axially loaded sandwich panels were performed. All tests are documented in the test reports D3.2 – part 3 [7] and D3.2 – part 4 [8]. In report D3.3 - part 4, the evaluation of the tests and additional numerical investigations are presented. A design procedure is developed The design model is based upon the existing design model for panels subjected to transverse loads according to EN 14509 [1] and the ECCS recommendations for the design of sandwich panels [2]. The existing model is extended in a way that consideration of axial forces and influences of 2nd order theory is possible. Also the behaviour due to long-term loads (creeping of the core material) can be considered by the design method presented in the report at hand.

The report at hand only deals with the global load bearing behaviour of axially loaded sandwich panels. Panels with openings are not covered. In addition the local load-bearing capacity at the areas of load application, i.e. the cut edges of the panel, is to be considered.

2 Load-bearing behaviour of panels subjected to transverse loads

In sandwich panels with flat and lightly profiled faces, bending moments are transferred by a force couple in both face sheets. In the face sheets, only normal tensile and compression stresses act.
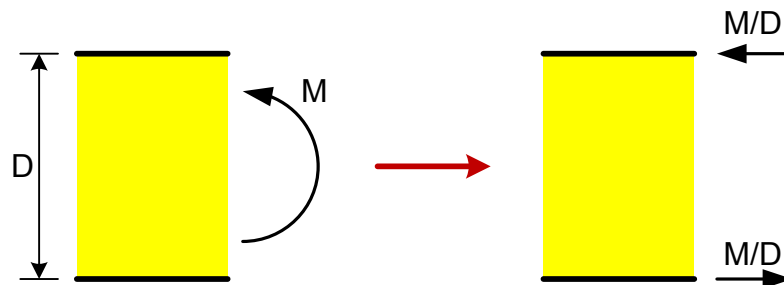

Fig. 2.1: **Load bearing behaviour of panels subjected to a bending moment**

The stress in the face sheets of a sandwich panel loaded by a bending moment M is

$$\sigma_F = \frac{M}{D \cdot A_F} \tag{2.1}$$

with

$A_F = B \cdot t_F$ cross sectional area of face sheet

t_F thickness of face sheer

B   width of panel

D   thickness of panel

The load bearing capacity is mostly restricted by reaching the ultimate stress in the compressed face sheet (Fig. 2.2). Failure by yielding of the face sheet subjected to tension occurs very rarely. The face sheet represents a plate which is elastically supported by the core material. The stability failure of the compressed face sheet is termed as wrinkling, the ultimate compression stress as wrinkling stress σ_w.

Fig. 2.2:　　　**Wrinkling of the compressed face sheet**

The elastic wrinkling stress of a plane elastically supported plate can be calculated according to the following equation [14].

$$\sigma_w = 0{,}82 \cdot \sqrt[3]{E_F \cdot E_C \cdot G_C} \tag{2.2}$$

with

E_F　　elastic modulus of face sheet (steel: E_F = 210.000 N/mm^2)

E_C　　elastic modulus of core material

G_C　　shear modulus of core material

According to [1] and [2] for design purposes the elastic wrinkling stress has to be reduced to take imperfections and quality of face, core and bonding between face and core into account. In the ECCS recommendations for sandwich panels [2] the following formulae is suggested.

$$\sigma_w = k \cdot \sqrt[3]{E_F \cdot E_C \cdot G_C} \tag{2.3}$$

with

k = 0,65 for continuously laminated polyurethane sandwich panels

k = 0,5....0,65 for other core materials and methods of manufacture

In EN 14509 k = 0,5 is given for all types of panels.

The experimentally determined wrinkling stress, however, often strongly deviates from the wrinkling stress calculated according to (2.3). Usually the wrinkling stress determined by testing is higher than the wrinkling stress determined by calculation. E.g. even a lightly lining of

the faces increases the wrinkling stress in comparison to the theoretical value. Therefore for design purposes the wrinkling stress is usually determined by bending tests.

The withstanding of transverse forces V is done by shear stresses in the core of the panel.

$$\tau_C = \frac{V}{A_C} \tag{2.4}$$

with

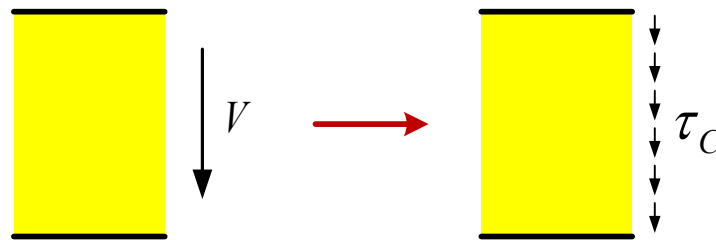$$A_C = B \cdot D \qquad \text{cross sectional area of the core}$$

Fig. 2.3:   **Load bearing behaviour of panels subjected to a transverse force**

When reaching the shear strength f_{Cv} of the core material shear failure occurs (Fig. 2.4).

Fig. 2.4:   **Shear failure of the core**

Because of the relatively soft core layer deflections caused by transverse forces have to be considered. So the deflection of a sandwich panel consists of a bending part w_b and a shear part w_v.

$$w = w_b + w_v = \int \frac{M\overline{M}}{B_S} \cdot dx + \int \frac{V\overline{V}}{GA} \cdot dx \tag{2.5}$$

with

bending stiffness:

$$B_S = E_F \cdot \frac{A_{F1} \cdot A_{F2}}{A_{F1} + A_{F2}} \cdot D^2 \tag{2.6}$$

shear stiffness:

$$GA = G_C \cdot A_C \tag{2.7}$$

For a single-span panel loaded by a uniformly distributed load q, the deflection w at mid-span is

$$w = w_b + w_v = \frac{5}{384} \cdot \frac{q \cdot L^4}{B_S} + \frac{1}{8} \cdot \frac{q \cdot L^2}{GA} \tag{2.8}$$

3 Load-bearing behaviour of axially loaded sandwich panels

3.1 Distribution of normal stresses

The stiffness of the faces is very much higher than the stiffness of the core material. This is why also for panels loaded by axial loads or by a combination from axial load and bending moment normal forces act only in the face sheets. In addition to normal stresses from the bending moment (force couple), compressive stresses from the axial load act in the face sheets Fig. 3.1.
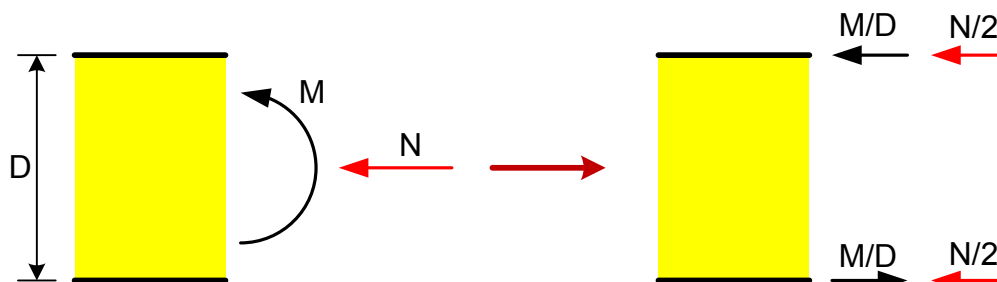

Fig. 3.1: **Load bearing behaviour for bending moment and axial force**

Also for panels with axial load failure can occur by wrinkling of the face sheet or by shear failure of the core material.

3.2 Global buckling

For slender building components loaded by axial compression forces global buckling can occur. Also for axially loaded sandwich panels this stability failure mode has to be considered. If an ideal panel without any imperfections is assumed, the axial load increases up to the elastic buckling load N_{cr}. Then, global buckling induces. Because of the deflection moments and transverse forces arise. The deflection strongly increases with a constant axial force. Also the stress resultants moment and transverse force increase. Finally, the wrinkling stress in mid-span or the shear strength at the support is reached and failure of the panels occurs [16], [17].

In Fig. 3.2 the load-deflection curve for an ideal panel as well as for an imperfect panel with initial deflection is shown.
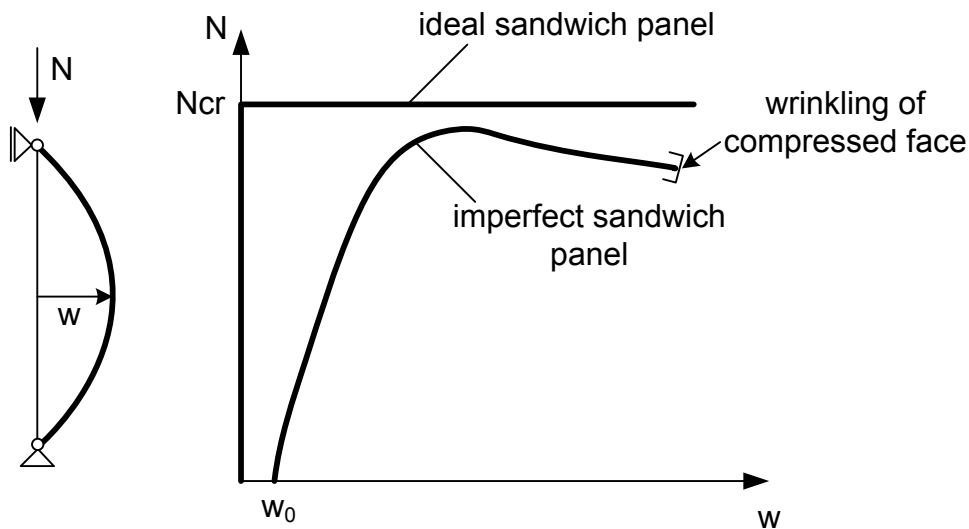

Fig. 3.2: **Load-deflection-diagram for axially loaded sandwich panels**

The elastic buckling load N_{cr} of a sandwich panel loaded by a centric axial load consists of the part N_{ki} considering the bending rigidity of the face sheets and the part GA considering the shear rigidity of the core. The rate N_{ki} corresponds to the elastic buckling load of both face sheets. The elastic buckling load of a sandwich panel can be calculated as follows

$$N_{cr} = \frac{N_{ki}}{1 + \dfrac{N_{ki}}{GA}}$$
(3.1)

$$\frac{1}{N_{cr}} = \frac{1}{N_{ki}} + \frac{1}{GA}$$
(3.2)

with

elastic buckling load due to bending rigidity

$$N_{ki} = \frac{\pi^2 \cdot B_S}{L^2}$$
(3.3)

elastic buckling load due to shear rigidity

$$GA = G_C \cdot A_C$$
(3.4)

The rate from bending rigidity N_{ki} on the elastic buckling load depends on the length of the panel, whereas the shear rate GA is independent of the length. With increasing length of the panel, the elastic buckling load of the sandwich panel approaches the rate N_{ki} from bending, i.e. the elastic buckling load of the face sheets. For very short panels the elastic buckling load

N_{cr} of the panel approaches the rate GA. Therefore GA represents an upper limit of the elastic buckling load (Fig. 3.3).
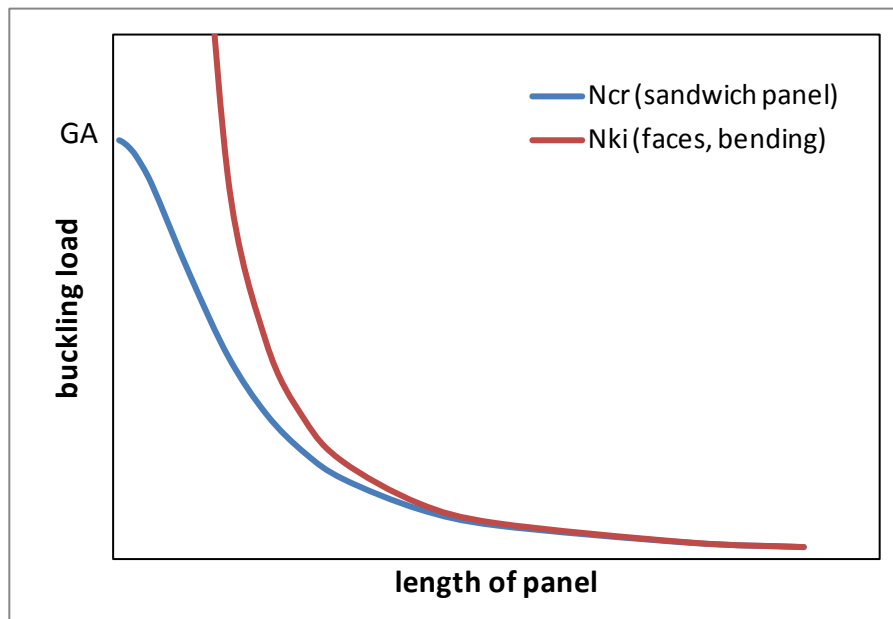

Fig. 3.3:   **Elastic buckling load of sandwich panels**

If imperfections and effects of 2nd order theory are neglected, the maximum compressive axial force of a centrically loaded panel corresponds to the axial load, which leads to wrinkling in both face sheets. The "axial wrinkling force" N_w can be calculated by the following equation.

$$N_w = \sigma_w \cdot (A_{F1} + A_{F2})$$
(3.5)

The "axial wrinkling force" N_w is comparable to the plastic normal force of a steel cross-section. Thus, the slenderness of a sandwich panel can be calculated as follows

$$\lambda = \sqrt{\frac{N_w}{N_{cr}}} = \sqrt{\lambda_{ki}^2 + \lambda_{GA}^2}$$
(3.6)

with

bending slenderness:

$$\lambda_{ki} = \sqrt{\frac{N_w}{N_{ki}}}$$
(3.7)

shear slenderness:

$$\lambda_{GA} = \sqrt{\frac{N_w}{GA}}$$
(3.8)

Corresponding to the rate from shear representing an upper limit of the elastic buckling load, the shear slenderness λ_{GA} represents a lower limit of the slenderness of a sandwich panel.

The first buckling mode of a sandwich panel loaded by a centric axial force corresponds to global buckling for a slenderness of the panel $\lambda > 1$. For $\lambda < 1$, the first buckling mode corresponds to wrinkling of the face sheets. In order that global buckling occurs, the panels must be thin and the faces must be relatively stiff, i.e. the face sheets must be thick. The global buckling load, however, is only reached for panels with rather unusual slenderness regarding building practice. For panels with usual dimension failure previously occurs by wrinkling or shear failure.

For (slender) components subjected to an axial compression force effects of 2nd order theory have to be considered in the design procedure. These result in an amplification of deflections and thus, also of the stress resultants moment and transverse force.

4   Buckling tests on axially loaded sandwich panels

For investigating the global load-bearing behaviour of axially loaded sandwich panels, buckling tests were performed. In order to be able to determine the global load-bearing capacity, local failure at load application area – e.g. by crippling of the face sheet – must be prevented. Therefore, the load was not introduced into the cut edges of the face sheets via contact such as in a real building structure. For load application, at first aluminium angles were stuck together with the face sheets and then fixed on a stiff load application plate. In order that the core of the panel can freely deform, the angles were stuck in a way that a gap of about 5 mm developed between the front side of the panel and the load application plate (Fig. 4.1).
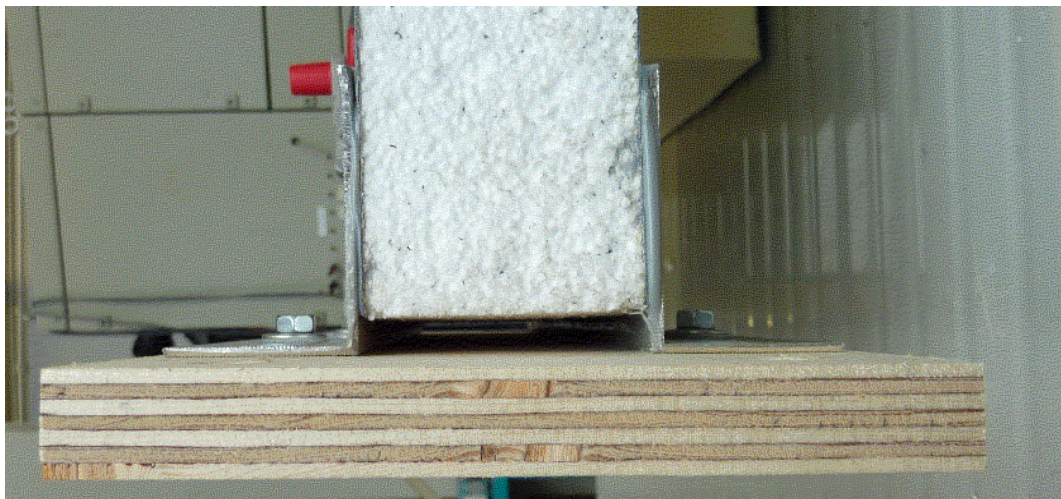

Fig. 4.1:   **Introduction of loads in the buckling tests**

In addition, panels with relatively big unusual slenderness regarding building practice were used for the tests. With increasing slenderness the influence of effects of 2nd order theory increases and global buckling and wrinkling occur more likely. Therefore, the tests are mainly used for verifying the FE-model and the assumptions made to develop the design model.

In the tests, the panel had a hinged support at each end (Fig. 4.3). At the beginning of the test, the panel was subjected to a deflection via an additional support in mid-span. In this deflected position the support was fixed for the remaining test period (Fig. 4.4). In a second step, the axial load was applied.
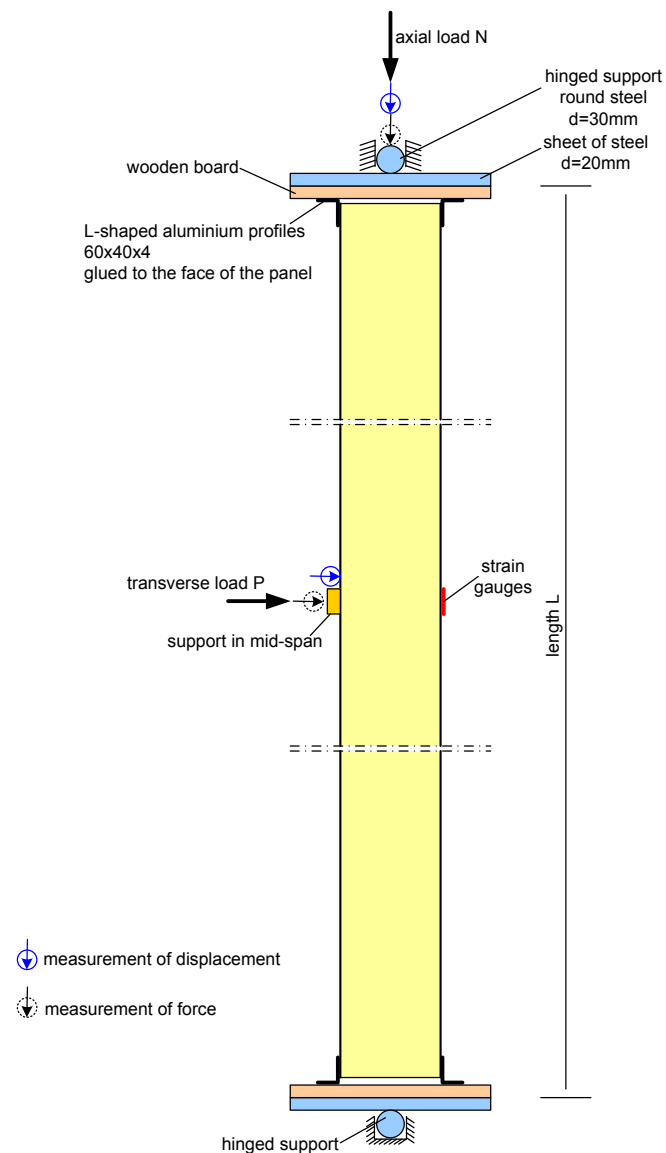

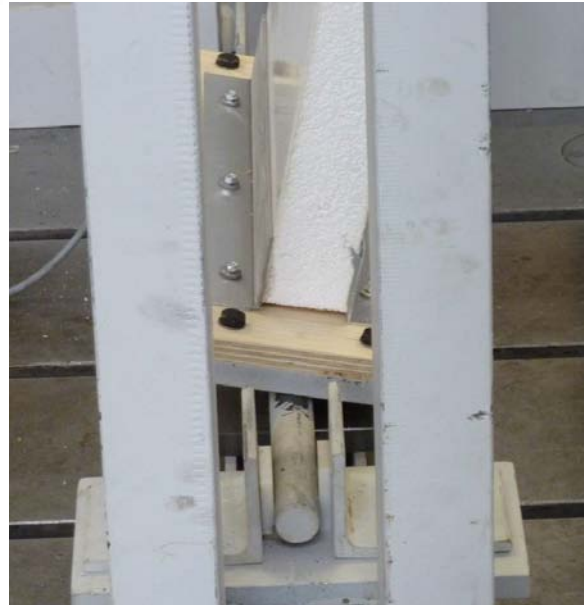**Fig. 4.2:** **Test set up for buckling tests**

Fig. 4.3: Hinged support

Fig. 4.4: Support at mid-span

In addition to the axial force and the deflection, the strain of the face sheet subjected to tension was measured. Therefore in mid-span strain gauges were applied (Fig. 4.5).
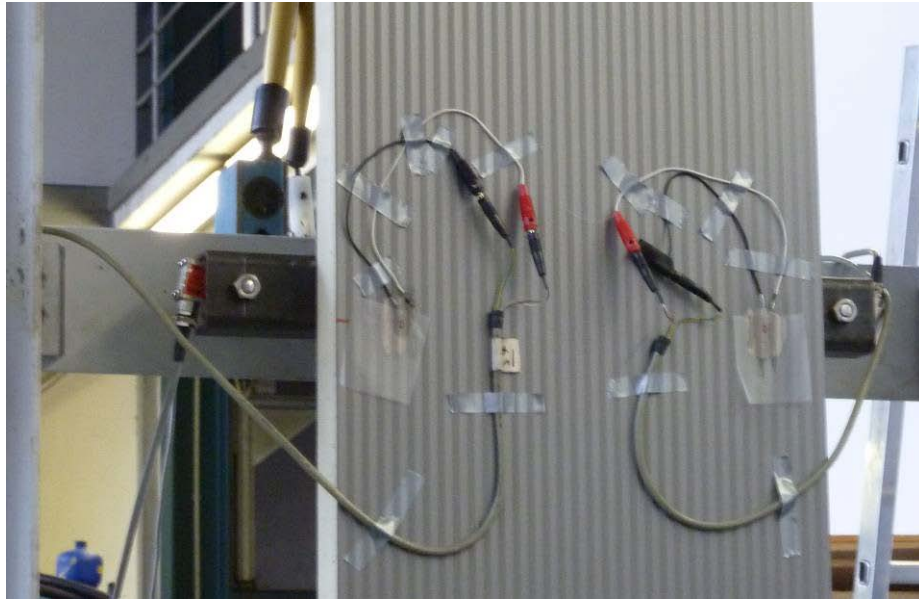
Fig. 4.5:   **Measurement of strain in mid-span**

If no failure previously occurs at load application area, the reaction force at the deflected mid-support decreases with increasing axial force. When roughly reaching the elastic buckling load the panel lifts from the fixed mid-support and the deflection increases without an essential change of the axial force (Fig. 4.6).
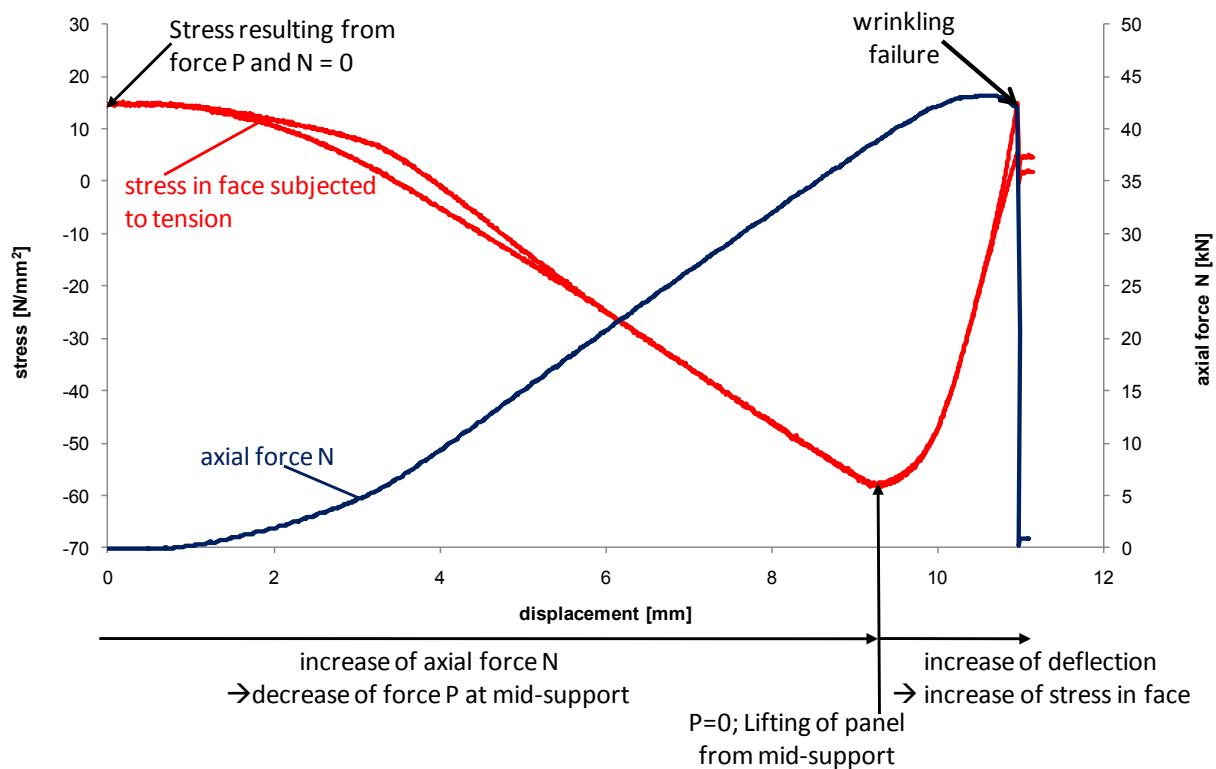

Fig. 4.6:   **Test performance of buckling tests (test no. 09)**

Because of the increasing deflection also the stress resultants moment and transverse force and thus the normal stress in the faces and the shear stress in the core increase. Finally failure occurs by wrinkling of the compressed face sheet or by shear failure of the core material.

Fig. 4.7:   **Increasing of deflection and wrinkling at mid-span**

In the buckling tests panels with different core materials and different faces were tested. Also the length of the tested panels and the initial deflection at mid-support were varied during the tests. A compilation of the performed buckling tests is given in Tab. 4.1. Tab. 4.2 shows a summary of the test results.

No.	type of panel *)	face	core	length of panel	initial deflection
01	F	steel, 0,75 mm	PU, 60 mm	2500 mm	15 mm
02	F	steel, 0,75 mm	PU, 60 mm	2500 mm	15 mm
03	L	GFRP, 1,8 mm	EPS, 60 mm	3000 mm	22 mm
04	K	steel, 0,60 mm	EPS, 60 mm	3000 mm	20 mm
05	F	steel, 0,75 mm	PU, 60 mm	3000 mm	15 mm
06	F	steel, 0,75 mm	PU, 60 mm	3000 mm	17,5 mm
07	F	steel, 0,75 mm	PU, 60 mm	3500 mm	20 mm
08	F	steel, 0,75 mm	PU, 60 mm	3500 mm	16,5 mm
09	F	steel, 0,75 mm	PU, 60 mm	3500 mm	5 mm

*) number refers to test report D3.2 [7], [8]

Tab. 4.1: **Performed buckling tests**

No.	max load [kN]	failure mode	final failure after global buckling	analytical buckling load [kN]
01	34,4	failure of glue at load introduction	-	58,8
02	51,0	delamination of face subjected to compression at load introduction	-	58,4
03	10,6	global buckling	failure of core near load introduction	10,4
04	25,3	failure of core near load introduction	-	63,5
05	46,2	global buckling	failure of core at load introduction	49,5
06	47,0	failure at load introduction	-	50,4
07	36,7	failure at load introduction	-	43,2
08	43,0	global buckling	failure of core at load introduction	42,0
09	43,4	global buckling	wrinkling of face	43,4

Tab. 4.2: **Results of buckling tests**

For each type of panel the material properties of core and face layers were determined (Tab. 4.3).

type of panel	thickness of face sheet [mm]	shear modulus of core [N/mm^2]	elastic modulus of core [N/mm^2]
F	0,698 / 0,700	3,81	3,66
K	0,554 / 0,551	5,57	-
L	GFRP (approx. 1,8 mm)	11,08	-

Tab. 4.3:   Material properties

For panel type F additional bending tests were performed to determine the wrinkling stress and the rigidity of the panel.

The buckling tests on axially loaded sandwich panels are documented in detail in D3.2-part 3 [7].

5   Numerical investigations

5.1   FE-Model

The numerical investigations were performed using the finite element program ANSYS. The face sheets of the panel were modelled with shell elements of type Shell 181. This element is defined by four nodes with three displacement degrees of freedom and three rotational degrees of freedom. It has bending, membrane and shear stiffness. As material behaviour, bilinear material equations were arranged (linear-elastic, ideal-plastic), i.e. after reaching the yield strength, yielding occurs without strain hardening.

The core layer of the panel was represented by volume elements of type Solid 185. This element has eight nodes with three displacement degrees of freedom. For the numerical investigations homogenous and isotropic core material was assumed.

The numerical investigations were performed on single-span panels with hinged supports. In order to be able to investigate the global load-bearing behaviour of the panels, failure at the load application areas must be prevented. Therefore, the support of the panels was modelled as illustrated in Fig. 5.1. Compared to the face sheets, a stiff plate is directly connected to both face sheets on the front side of the panel. The core of the panel and the plate has no sheared nodes, so the core can freely deform. This corresponds to the construction of the support in the buckling tests, where free deformation of the core was facilitated by a gap between core material and load application plate. On the base point, displacements were prevented at a line of nodes; this corresponds to a hinged support. At the opposite end of the panel, the nodes are only constrained horizontally, but they are vertically displaceable. On these nodes, the axial load can either be applied as load or as displacement.
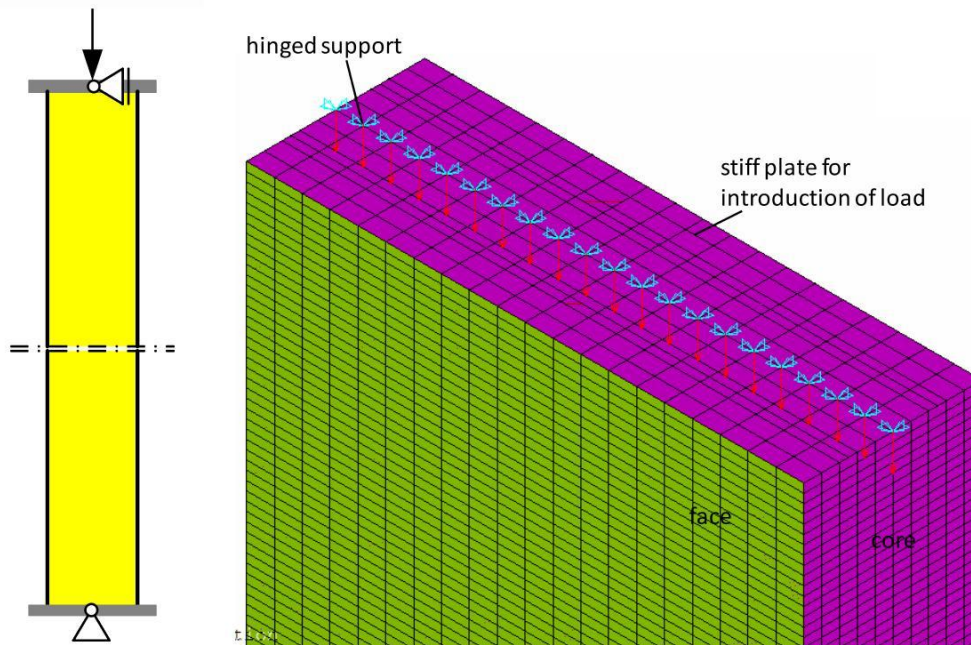
Fig. 5.1: FE-model and detailed view on the support

5.2 Preliminary investigations

5.2.1 Preliminary remark

For checking the efficiency of the FE model preliminary investigations were performed. At first, the necessary fineness of the mesh was defined. Especially if wrinkling of the face sheet has to be represented by the model, the element size in longitudinal direction of the sandwich panel has a decisive influence on the results. The mesh must be so fine that the waves corresponding to the eigenmode of a wrinkled face sheet can correctly be represented. For the performed investigations a length of 4 mm was sufficient, the thickness direction resulted in a necessary mesh length of about 10 mm, the width direction in about 20 mm.

The FE model was checked by comparing results of the numerical calculation with analytical values. For this purpose, the stiffness for bending load and different eigenvalues, e.g. elastic wrinkling stress and elastic buckling load were considered. In addition, some of the buckling tests were recalculated.

5.2.2 Rigidity of the panel

In order to examine, whether the FE-model correctly represents the rigidity of a sandwich panel, the deflection determined in the FE-analyses was compared with the analytically determined deflection according to (2.8). In addition, the analytically and numerically determined stresses in the face sheets were compared to each other.

In the numerical investigations the panel was loaded by a uniform transverse load which was selected in a way that the stress in the face sheets was about 100 N/mm^2.

With the parameters E_F = 210000 N/mm^2, G_C = 2 N/mm^2, t_F = 0,6 mm, B = 250 mm and a thickness range of 40 mm to 100 mm the following analytical and numerical results of stress σ_F and deflection w were calculated.

Length	Thick-ness	load	analytical results				FE		deviation	
			w_b	w_v	w	stress	w	stress	w	stress
[mm]	[mm]	[N/mm^2]	[mm]	[mm]	[mm]	[N/mm^2]	[mm]	[N/mm^2]	[%]	[%]
3000	100	0,0053	8,9	30,0	38,9	100	39,4	99,8	1,21	0,20
	80	0,0043	11,2	30,0	41,2	100	41,4	99,9	0,58	0,10
	60	0,0032	14,9	30,0	44,9	100	44,8	99,9	0,18	0,10
	40	0,0021	22,3	30,0	52,3	100	52,0	99,9	0,61	0,10
2000	100	0,0080	4,0	30,0	34,0	100	35,3	99,9	3,92	0,10
	80	0,0064	5,0	30,0	35,0	100	35,5	99,9	1,54	0,10
	60	0,0048	6,6	30,0	36,6	100	36,6	99,9	0,04	0,10
	40	0,0032	9,9	30,0	39,9	100	39,5	99,9	1,05	0,10

Tab. 5.1:   **Comparison of analytical and numerical results**

Based on the good agreement between analytical and numerical analysis, it can be assumed that the FE-model correctly reproduces the bending behaviour of a sandwich panel.

5.2.3 Buckling behaviour

In addition, the FE-model was checked by comparison of numerically and analytically determined eigenvalues. For this purpose, the wrinkling stress for panels subjects to bending and axial load and the global buckling load were considered.

<u>Wrinkling stress due to bending</u>

For panels subjected to a constant transverse load the first eigenvalue was determined by numerical analysis, and the corresponding stress in the face sheets was calculated. These stresses are compared to the wrinkling stress calculated according to (2.2). For the parameters G_C =3 N/mm^2, E_C = 4 N/mm^2, t_F = 0,5 mm and a thickness range of 40 mm to 100 mm, the following results ensue.

Thickness [mm]		40	60	80	100
length [mm]		2000	3000	3000	3000
wrinkling stress σ_w	FE	111,6	111,6	111,6	111,6
	analytical	112,5	111,6	111,6	111,6
deviation [%]		0,77	0,03	0,02	0,01

Tab. 5.2:   **Comparison of analytical and numerical results for wrinkling stress**
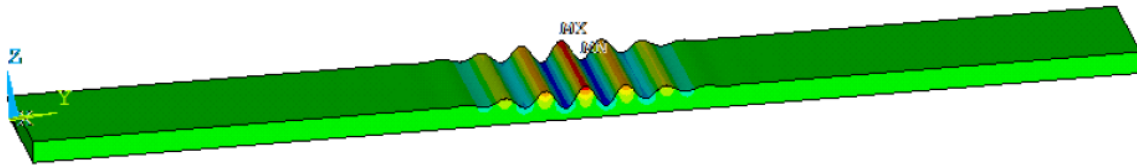
Fig. 5.2: **Wrinkling of the compressed face (buckling mode)**

Wrinkling stress due to centric axial load

For panels with a slenderness $\lambda < 1$ the first eigenmode upon centric axial load corresponds to wrinkling of both face sheets. The corresponding axial wrinkling force N_w can be calculated according to (3.5) and (2.2).

In the FE analysis, the panel was loaded in longitudinal direction at the nodes forming the displaceable support. For a panel with the parameters given in the previous section, the following values result from the analytical and numerical analysis.

Thickness [mm]		40	60	80	100
Length [mm]		600	2000	2000	2000
N_w	FE	27897	27897	27897	27897
	analytical	26975	27821	27470	27788
deviation [%]		3,3	0,3	1,5	0,4

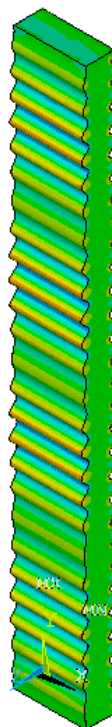**Tab. 5.3:** **Comparison of analytical and numerical results for axial wrinkling load N_w**

Fig. 5.3: **Wrinkling caused by axial load (eigenvalue)**

Elastic buckling load for global buckling

For panels with slenderness's $\lambda > 1$, the first eigenmode is global buckling of the panel. The analytical eigenvalue can be calculated according to (3.1) and (3.2). For the parameters $G_C = 2$ N/mm^2, $E_C = 4$ N/mm^2, $t_F = 0,7$ mm and a thickness range of 40 mm to 100 mm the following numerical and analytical results ensue for the global buckling load N_{cr}.

Thickness [mm]		40	60	80	100
Length [mm]		3000	3000	3500	4500
N_{cr}	FE	12344	21223	28126	32086
	analytical	12415	21263	27994	31579
deviation [%]		0,6	0,2	0,5	1,6

Tab. 5.4: **Comparison of analytical and numerical results for global buckling load**

Fig. 5.4: **Global buckling caused by axial load (eigenvalue)**

For all results listed above, a very good agreement between analytically and numerically determined eigenvalues can be observed.

5.2.4   Comparison to test results

In addition to the verification of the FE-model by comparison to analytical values, the model was also checked by comparison to test results. For the numerical calculations, the thickness of the face sheets and the material properties of the core determined for the tested panels were used.

The correct representation of the rigidity was checked by comparison with the bending test performed within the framework of the tests on axially loaded sandwich panels [7]. In the fol-

lowing figure, the force-deflection relationships determined in the test and in the numerical analysis are opposed to each other.
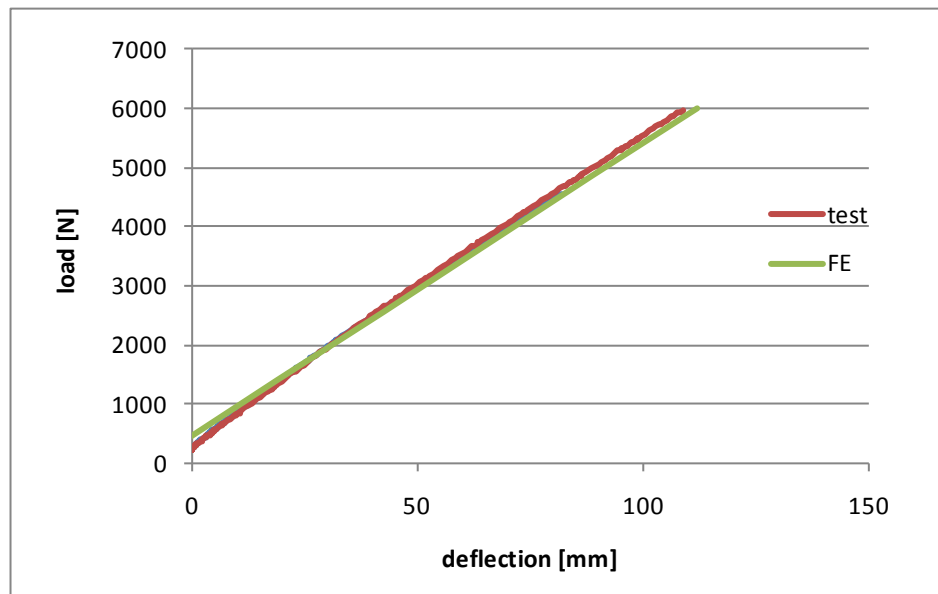

Fig. 5.5: **Load-deflection-diagram for test and FE-calculation**

In addition, some of the buckling tests documented in [7] were recalculated in order to verify the FE-model. In doing so, tests were selected for which the axial force could be increased up to the buckling load without failure at the load application area, i.e. the tests in which lifting of the panel from the mid-support and thus, an increase of deflection took place (tests no. 03, 05, 08, 09).

At the mid-support only compression forces, but no tensile forces are transferred. In the FE model, the mid-support was represented by longitudinal springs (element type combin39) (Fig. 5.7). The load-displacement relationship of the springs was selected in a way that they have a high stiffness, if compression forces act, but they cannot transfer any tensile forces (Fig. 5.6).
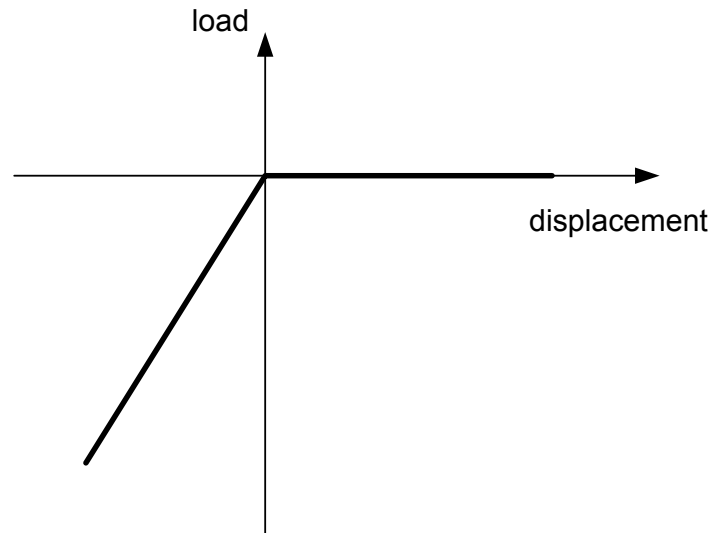
load

displacement

Fig. 5.6: **Load-displacement-relationship for springs at mid support**

support at mid-span
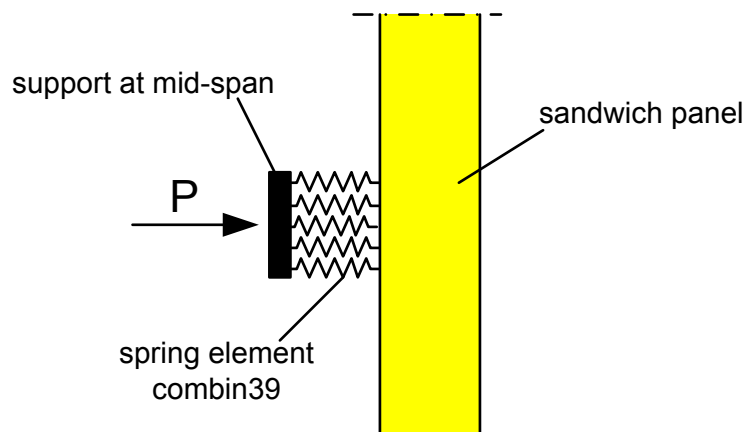
sandwich panel

P

spring element
combin39

Fig. 5.7: **Mid-support in the FE-model**

In the following table, the maximum loads determined in the tests are opposed to the maximum loads from the numerical calculation. There is a good agreement between test and numerical calculation.

test No.	result of test	result of FE	deviation	analytical buckling load
03	10,6 kN	10,6 kN	0,4 %	10,40 kN
05	46,2 kN	45,1 kN	2,4 %	49,5 kN
08	43,0 kN	42,5 kN	1,2 %	42,0 kN
09	43,4 kN	42,6 kN	1,8 %	43,4 kN

Tab. 5.5: **Comparison of test results and numerical calculation**

5.3   Calculations for determination of ultimate stress

For the design of panels subjected to transverse loads the wrinkling stress σ_w is the ultimate compression stress, which can act in a face sheet. It is determined in bending test. In order to determine the ultimate stress for panels loaded by an axial force or by a combination of axial load and transverse load, FE-analyses were performed. For this purpose, the panels were loaded by a centric axial compression load or a combination of an axial load and a constant transverse load. The transverse load was selected in a way that the compressive stress caused by bending corresponds to about half the wrinkling stress. In addition, calculations with panels with a global initial deflection and a centric axial load were done. As global imperfection an initial deflection e_0 corresponding to the first eigenmode of an axially loaded panel was applied (Fig. 5.8). The range of the initial deflection e_0 was selected according to the maximum allowable longitudinal bowing following EN 14509 [1].

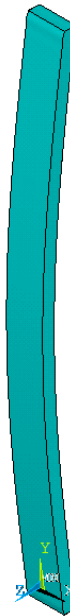$$e_0 = \frac{1}{500} \cdot L \tag{5.1}$$

Fig. 5.8:   **Global imperfection for numerical calculation**

For all calculations, a local geometric imperfection was applied on the face sheet subjected to compression. The local imperfection corresponds to the eigenmode when reaching the wrinkling stress (Fig. 5.9).
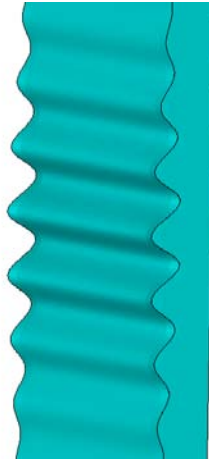
Fig. 5.9: Local imperfection for numerical calculation

The calculations were performed for the panel types given in Tab. 5.6. The range of the local imperfection was varied between $0,05 \cdot t_F$ and $0,1 \cdot t_F$.

Type of panel		P1	P2	P3
E_C	[N/mm^2]	8	6	4
G_C	[N/mm^2]	4	3	2
t_F	[mm]	0,6	0,5	0,7
D	[mm]	80	60	100

Tab. 5.6: Panels for calculation of ultimate stress

Calculations on the load-bearing capacity were performed in order to determine the ultimate compressive stress. For comparison, calculations on the load-bearing capacity were carried out on panels with the same local imperfections under bending load only and the ultimate compression stress was determined as well. This stress corresponds to the wrinkling stress, which is usually determined by bending tests. Fig. 5.10 shows a comparison of the numerically determined ultimate stresses for different kinds of loadings.
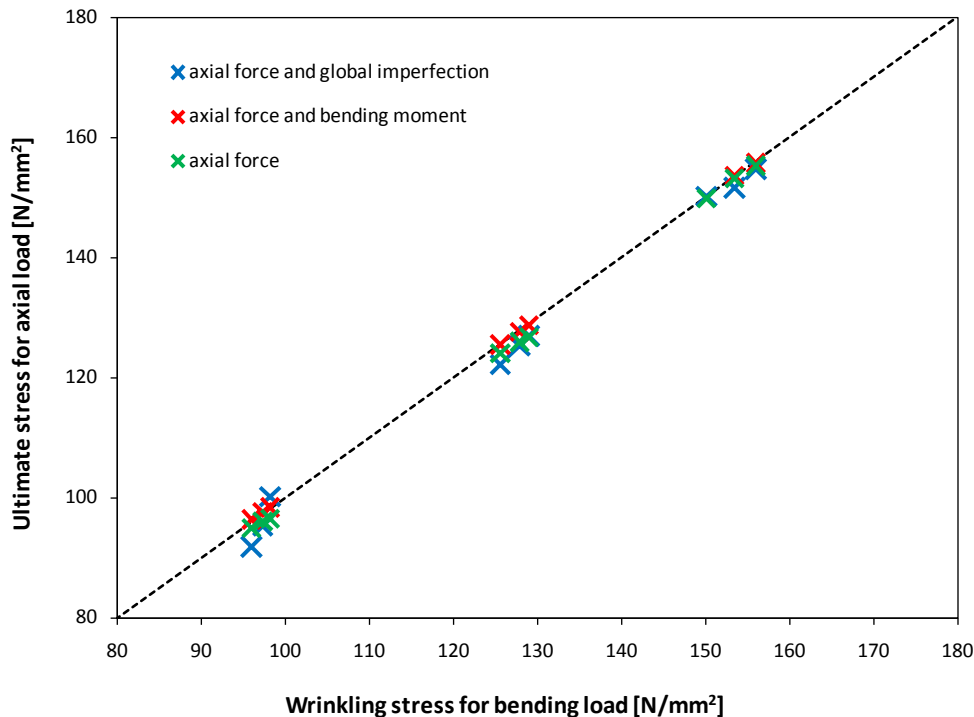
Fig. 5.10:   **Comparison of ultimate stresses**

Obviously, the failure stress upon normal forces or combined load from normal force and bending moment and the failure stress for pure transverse load are identical. Therefore, the wrinkling stress used to design panels subjected to transverse loads can also be used to design axially loaded sandwich panels.

This assumption was confirmed by the tests carried out on axially loaded sandwich panels. In one of the buckling tests (test no. 09, [7]) failure occurred by wrinkling of the face sheet subjected to compression (Fig. 5.12). The stresses in the face sheets were calculated from the axial load and the deflection measured in the test. The stress in the compressed face sheet was 163 N/mm^2 upon failure of the panel (Fig. 5.11). For the corresponding face sheet, the wrinkling stress was also determined in a bending test on a panel of the same type (Fig. 5.12). The wrinkling stress for transverse load was 165 N/mm^2. This good agreement confirms the applicability of the wrinkling stress determined by bending tests as ultimate stress for axially loaded panels.
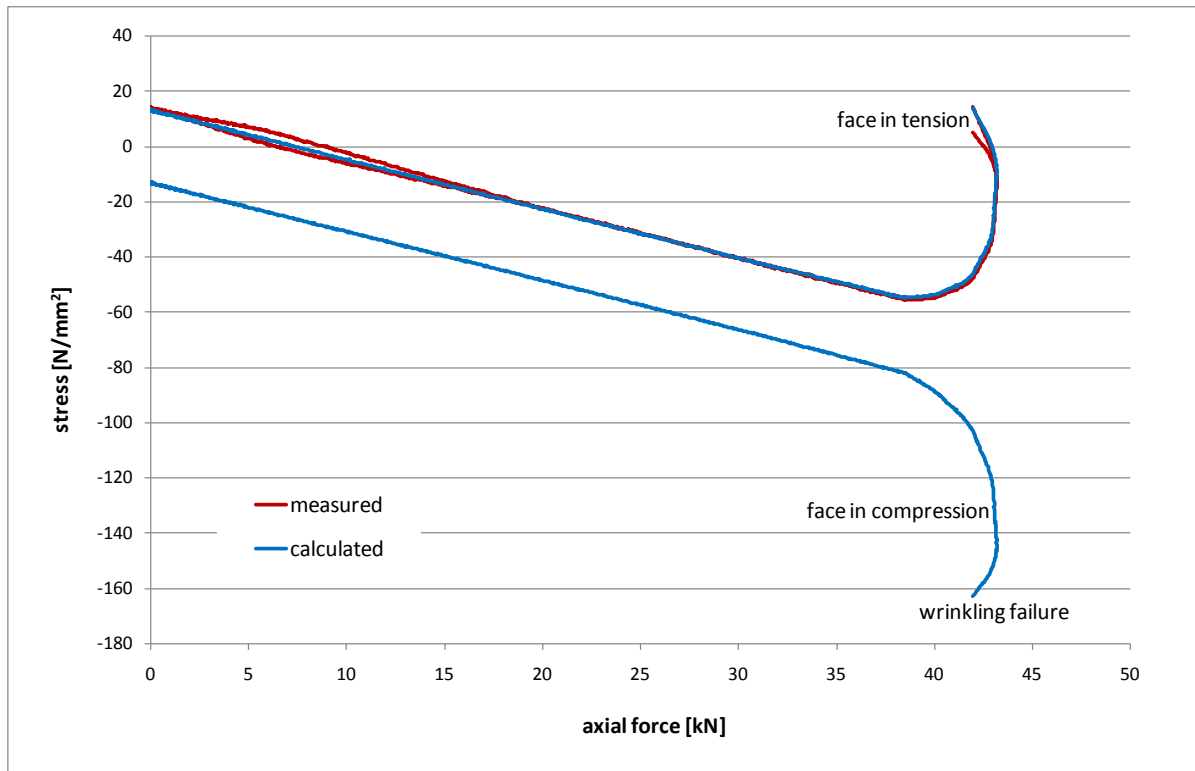
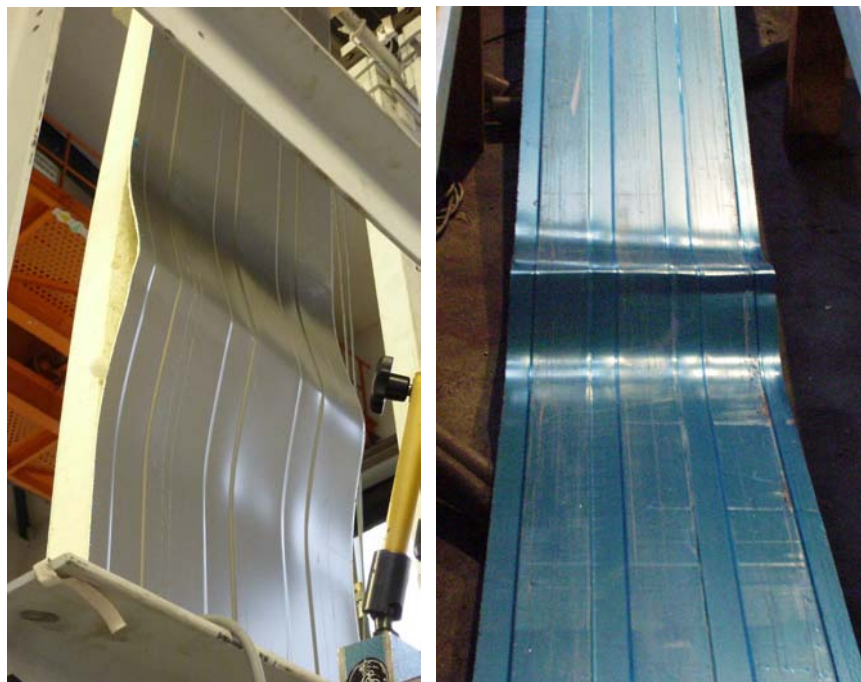**Fig. 5.11:** **Measured and calculated stresses in the buckling test**

Fig. 5.12: **Wrinkling of the compressed face in buckling and bending test**

5.4   Calculations to investigate the influence of 2nd order theory

If components are loaded by compressive axial loads, effects of 2nd order theory have to be taken into account, i.e. deformations are considered in determination of stress resultants. If stress resultants are determined according to 1st order theory deformations are neglected.

Because of effects of 2nd order theory stresses do not increase proportionally to the axial load. Due to the axial force an increase of deflection also results in an increase of moment and transverse force.

The amplification of the stress resultants moment M and transverse force V as well as the amplification of the deflection w can approximately be determined by the amplification factor α.

$$M^{II} = \alpha \cdot M^{I} \tag{5.2}$$

$$V^{II} = \alpha \cdot V^{I} \tag{5.3}$$

$$w^{II} = \alpha \cdot w^{I} \tag{5.4}$$

$$N^{II} = N^{I} \tag{5.5}$$

with

M^{I}, V^{I}, w^{I} stress resultants and deflection according to 1st order theory

M^{II}, V^{II}, w^{II} stress resultants and deflection according to 2nd order theory

amplification factor:

$$\alpha = \frac{1}{1 - \dfrac{N}{N_{cr}}} \tag{5.6}$$

If effects of 2nd order theory are considered, also geometrical imperfections such as initial deflections must be considered for determination of stress resultants. So the moment according to 1st Order Theory is

$$M^{I} = M^{0} + N \cdot e_{0} \tag{5.7}$$

M^{0} moment caused by transverse load and fixed-end moment

$N \cdot e_{0}$:   moment caused by initial deflection in conjunction with axial force

In order to check whether the approximation by the amplification factor α can also be applied for sandwich panels, FE-analyses were carried out and the load-deflection relationships were compared to the curves calculated according to the equations given above. In Fig. 5.13 and Fig. 5.14, the load-deflection curves from FE-analyses are opposed to the corresponding curves determined with the amplification factor α.
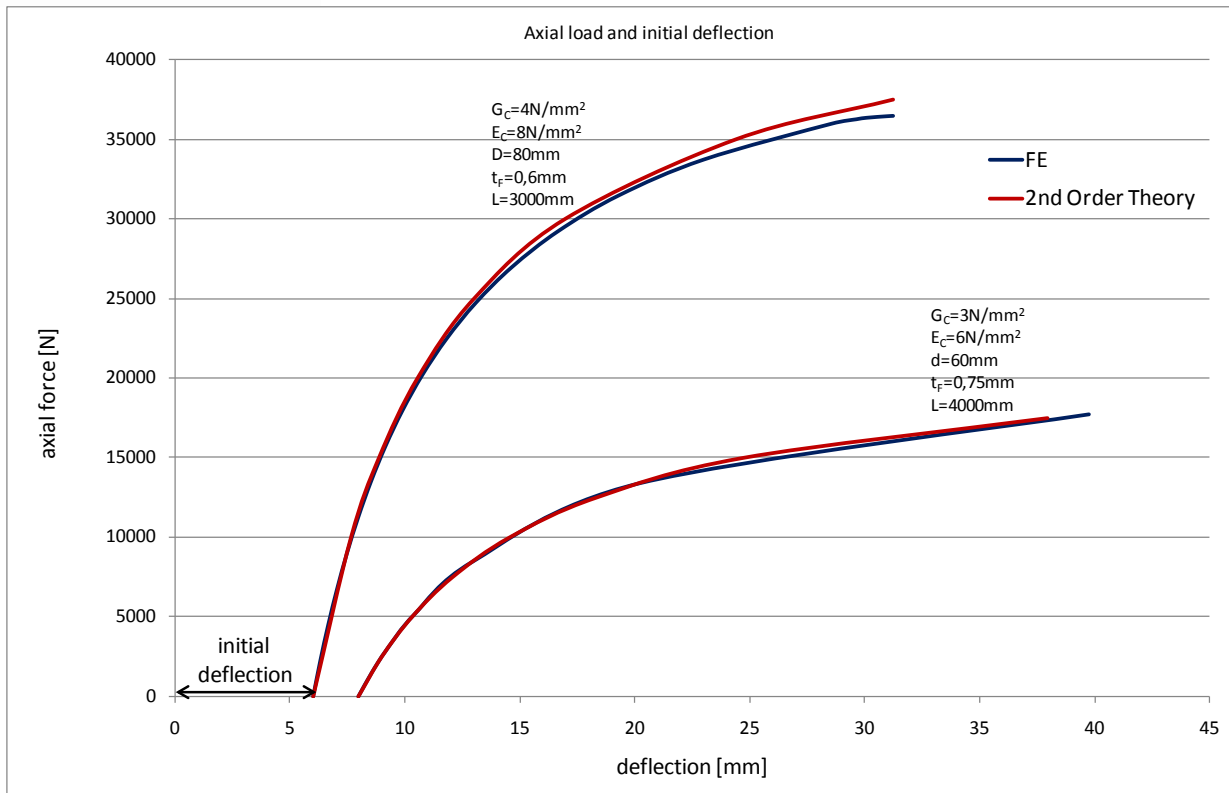
Fig. 5.13: Load-deflection-curves for FE and calculation by 2nd Order Theory
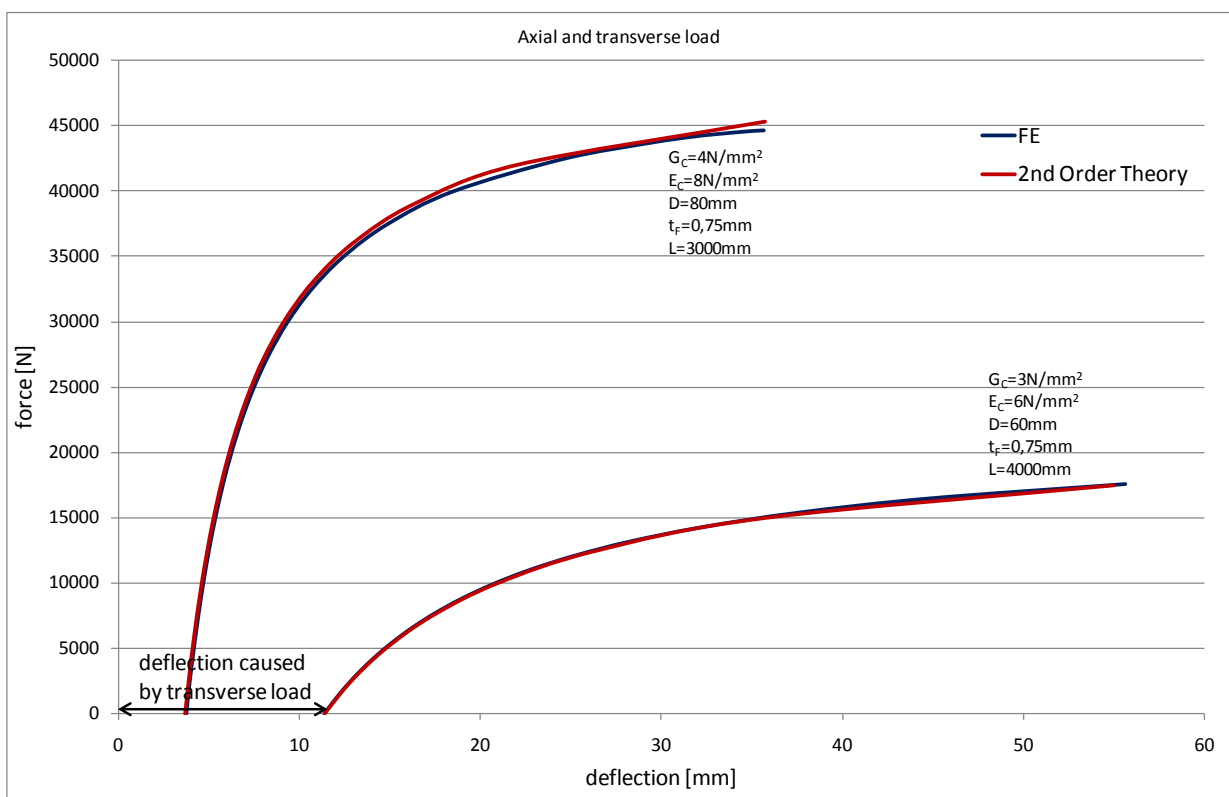

Fig. 5.14: Load-deflection- curves for FE and calculation by 2nd Order Theory

The applicability of the amplification factor α on axially loaded sandwich panels was also con-
firmed by the buckling tests. The stresses in the face sheets were calculated in dependence

on the axial force and compared to the stresses determined from the measured strains. For selected tests, the calculated and the measured stresses are compared to each other (Fig. 5.15 to Fig. 5.17). Also in this case, a good agreement between test and calculation by 2nd Order Theory can be observed.
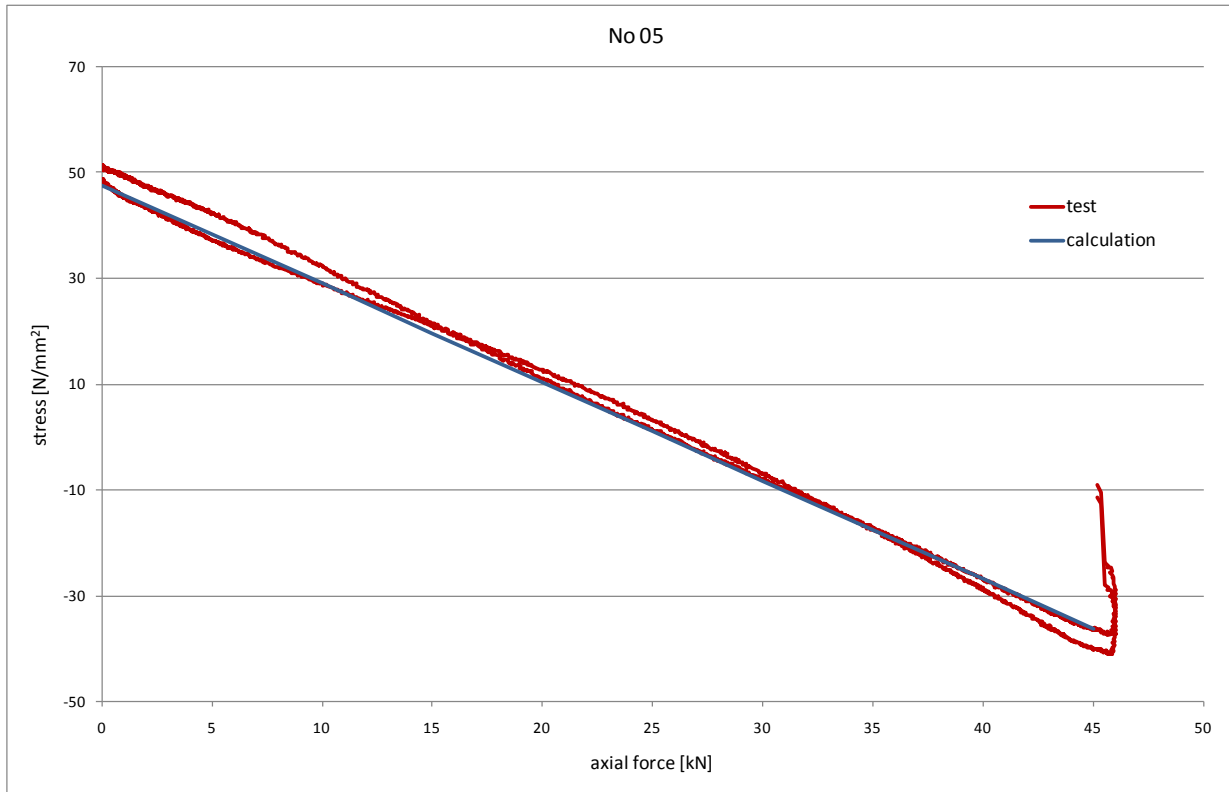

Fig. 5.15: **Comparison between test and calculation by 2nd Order Theory, test 05**
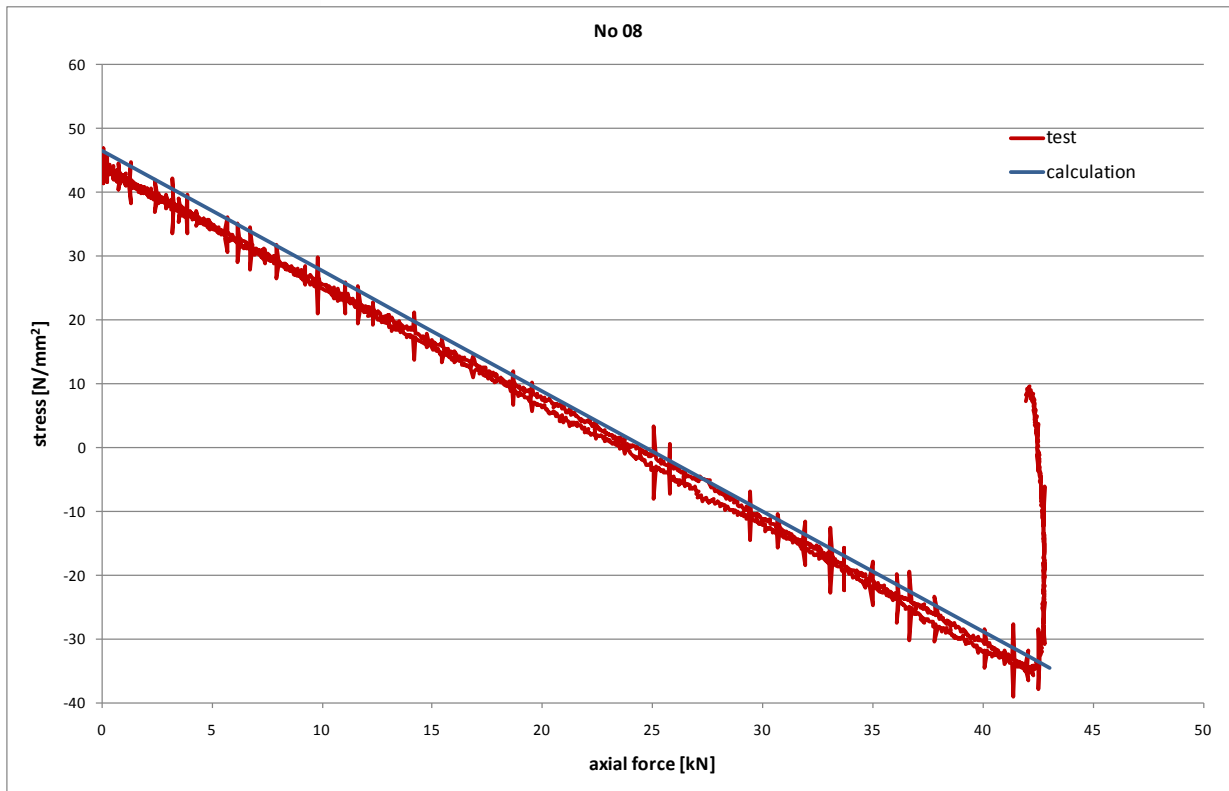
Fig. 5.16: Comparison between test and calculation by 2nd Order Theory, test 08
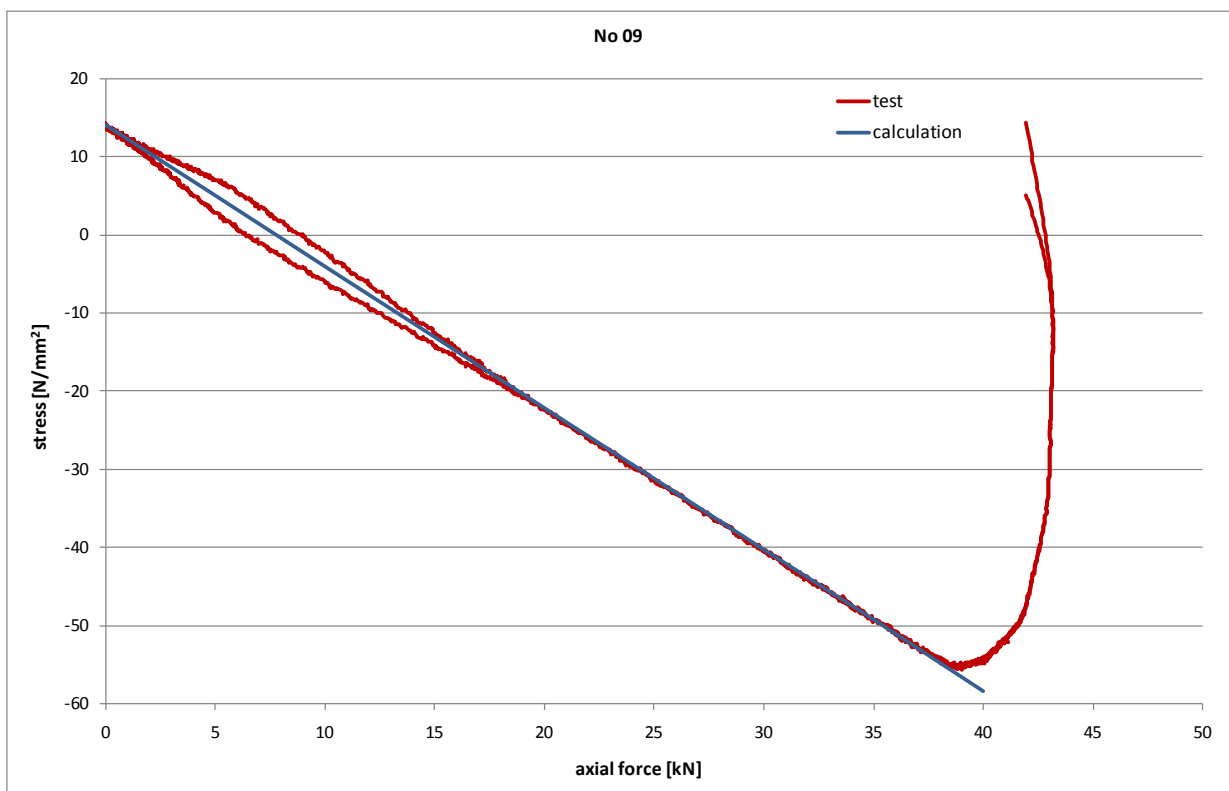

Fig. 5.17: Comparison between test and calculation by 2nd Order Theory, test 09

In [12], the approximate calculation with the amplification factor α is compared with the exact analytical solution by means of an example. Also in this case, the results agree well.

6 Design methods

6.1 General

The influence of an axial load can be considered either by design according to 2nd order theory or by design according to equivalent member method. For design according to 2nd order theory the stress resultants moment and transverse force determined according to 1st order theory are increased by the amplification factor α. In addition, geometrical imperfections must be considered for the determination of stress resultants, since they also result in moments and transverse forces if an axial force exists. Finally, the panels are designed on stress level.

For design according to equivalent member method, the stress resultants according to the 1st order theory are used. In dependence on the geometric imperfection and the slenderness of the component, however, the maximum compressive axial force (axial wrinkling force N_w) has to be reduced.

6.2 Design according to 2nd order theory

The stress resultants according to 2nd order theory are determined by approximation by amplification of the stress resultants according to 1st order theory.

In addition to moments from transverse load (e.g. wind loads) and fixed-end moments, also geometrical imperfections must be considered in the moment according to 1st order theory. As geometrical imperfection an initial deflection e_0 can be applied. The range of this imperfection can be selected according to the maximum allowable longitudinal bowing following EN 14509 [1].

$$e_0 = \frac{1}{500} L \tag{6.1}$$

Also deflections w_T from a temperature difference ΔT between internal face and external face result in moments and transverse forces if the panel is axially loaded. These moments can be determined just as the moments from geometrical imperfections.

$$M_T^I = N \cdot w_T \tag{6.2}$$

$$w_T = \Delta T \cdot \frac{\alpha_F \cdot L^2}{D \cdot 8} \tag{6.3}$$

α_F coefficient of thermal expansion

So the stress resultants according to 2nd order theory are calculated as follows.

$$M^{II} = \alpha \cdot M^I \tag{6.4}$$

$$V^{II} = \alpha \cdot V^I \tag{6.5}$$

$$N^{II} = N^I \tag{6.6}$$

amplification factor:

$$\alpha = \frac{1}{1 - \dfrac{N}{N_{cr}}}$$

(6.7)

$$M^I = M^0 + N \cdot e_0 + N \cdot w_T$$

(6.8)

M^0 moment caused by transverse load and fixed-end moment (N·e)

$N \cdot e_0$:   moment caused by initial deflection in conjunction with axial force

$N \cdot w_T$:   moment caused by temperature deflection

After determination of moment and transverse force according to 2nd order theory, design is done on the stress level using the wrinkling stress as ultimate stress.

$$\sigma_F = \frac{N}{A_{F1} + A_{F2}} + \frac{M^{II}}{A_{F1} \cdot D} \leq \sigma_w$$

(6.9)

For transverse load, the shear strength f_{Cv} of the core material can also become decisive.

$$\tau_C = \frac{V^{II}}{A_C} \leq f_{Cv}$$

(6.10)

Since the wrinkling stress σ_w and the shear strength f_{Cv} are usually determined by testing, local imperfections of the panels such as surface irregularities of the face sheet and the material properties of the core are already considered in the ultimate stress.

6.3 Design according to the equivalent member method

Alternative to the design according to 2nd order theory on the stress level also design by equivalent member method is possible. For determining the reduction factor of the axial wrinkling force N_w a buckling curve for the corresponding sandwich panel is necessary. For a centrically loaded panel with the initial deflection e_0 we get the following equation. This equation considers the stress resultants according to 2nd order theory. The ultimate stress of the compressed face sheet is the wrinkling stress σ_w.

$$\frac{N}{(A_{F1} + A_{F2}) \cdot \sigma_w} + \frac{N \cdot e_0}{D \cdot A_{F1} \cdot \sigma_w} \cdot \frac{1}{1 - \dfrac{N}{N_{cr}}} \leq 1$$

(6.11)

Insertion of the axial wrinkling force N_w and the slenderness λ as well as the reduction factor

$$\chi = \frac{N}{N_w}$$

(6.12)

results in the equation

$$\chi + \frac{2 \cdot e_0}{D} \cdot \frac{\chi}{1 - \chi \cdot \lambda^2} = 1 \qquad (6.13)$$

As solution of (6.13) the known formula for determining the reduction factor is obtained.

$$\chi = \frac{1}{\phi + \sqrt{\phi^2 - \lambda^2}} \qquad (6.14)$$

with

$$\phi = 0,5 \cdot \left[1 + \frac{2 \cdot e_0}{D} + \lambda^2\right] \qquad (6.15)$$

By application of the length-dependent initial deflection

$$\overline{e}_0 = \frac{e_0}{L} \qquad (6.16)$$

(6.15) can be transformed to

$$\phi = 0,5 \cdot \left(1 + \alpha \cdot \sqrt{\lambda^2 - \lambda_{GA}^2} + \lambda^2\right) \qquad (6.17)$$

with the imperfection factor

$$\alpha = \frac{2 \cdot \overline{e}_0}{D} \cdot \pi \cdot \sqrt{\frac{B_S}{N_w}} \qquad (6.18)$$

The imperfection factor depends on the geometry of the panel (thickness D, bending rigidity B_S). In addition, the geometrical imperfection $\overline{e}_0$ is considered in α. By consideration of the axial wrinkling force N_w and thus, the wrinkling stress σ_w also local imperfections as well as material properties of the core layer are indirectly considered in the imperfection factor.

As an example, Fig. 6.1 shows a buckling curve for a sandwich panel. For checking the method, additionally some reduction factors determined by FE-analyses are shown in the figure.
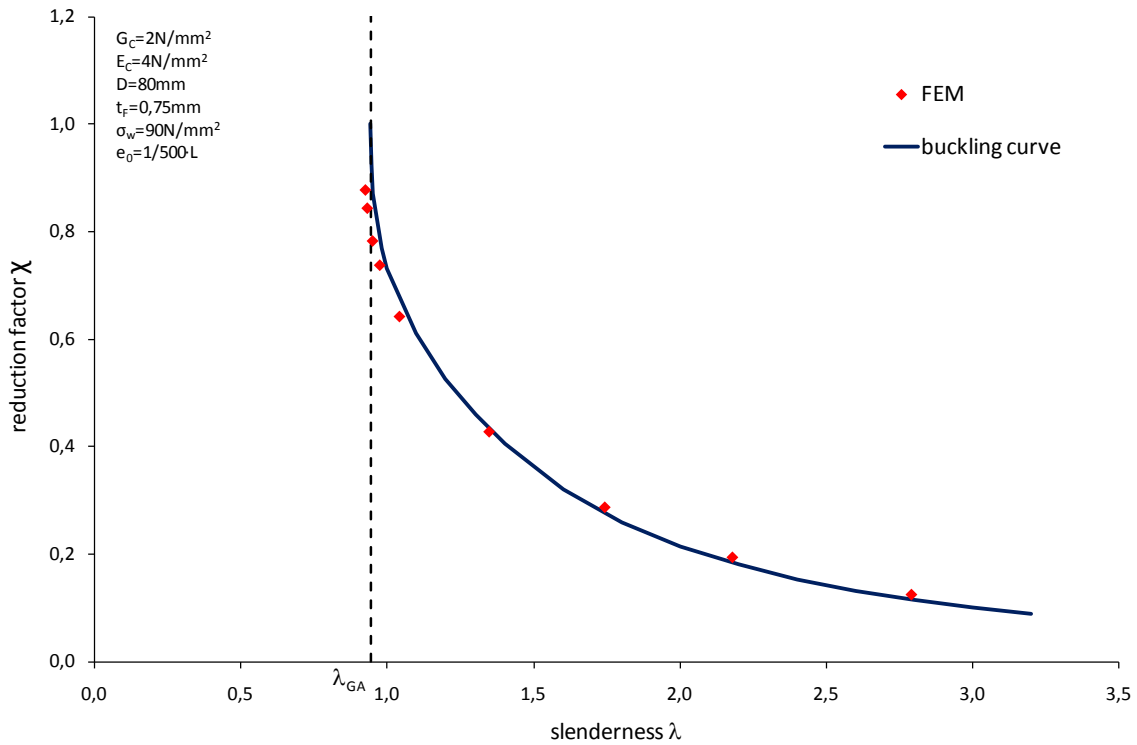
G_C=2N/mm²
E_C=4N/mm²
D=80mm
t_F=0,75mm
σ_w=90N/mm²
e_0=1/500·L

Fig. 6.1: **Example of a buckling curve for sandwich panels**

In order to be able to consider also moments from transverse load or eccentric axial loads, besides a practically never existing pure centric axial load, the above equation can be extended by a part for the bending moment following EN 1993-1-1 (section 6.3 and annex B).
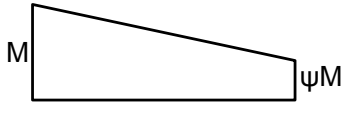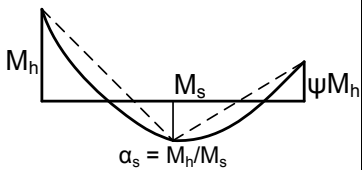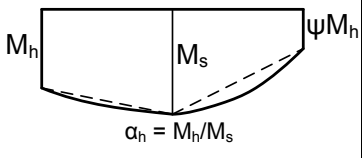
$$\frac{N}{\chi \cdot N_w} + k_{yy}\frac{M}{M_w} \le 1 \tag{6.19}$$

with

$$M_w = D \cdot A_F \cdot \sigma_w \tag{6.20}$$
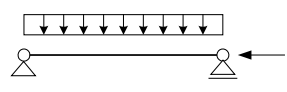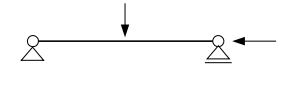
$$k_{yy} = C_{my} \cdot (1 + 0,8 \cdot \frac{N}{\chi \cdot N_w}) \tag{6.21}$$

C_{my}: equivalent uniform moment factor according to EN 1993-1-1, table B.3 (Tab. 6.1)

moment distribution			C_{my}	
			uniformly distributed load	point load
M ... ψM	$-1 \le \psi \le 1$		$0,6+0,4\psi \ge 0,4$	
M_h ... M_s ... ψM_h $\alpha_s = M_h/M_s$	$0 \le \alpha_s \le 1$	$-1 \le \psi \le 1$	$0,2+0,8\alpha_s \ge 0,4$	$0,2+0,8\alpha_s \ge 0,4$
	$-1 \le \alpha_s < 0$	$0 \le \psi \le 1$	$0,1-0,8\alpha_s \ge 0,4$	$-0,8\alpha_s \ge 0,4$
		$-1 \le \psi < 0$	$0,1(1-\psi)-0,8\alpha_s \ge 0,4$	$0,2(-\psi)-0,8\alpha_s \ge 0,4$
M_h ... M_s ... ψM_h $\alpha_h = M_h/M_s$	$0 \le \alpha_h \le 1$	$-1 \le \psi \le 1$	$0,95+0,05\alpha_h$	$0,90+0,10\alpha_h$
	$-1 \le \alpha_h < 0$	$0 \le \psi \le 1$	$0,95+0,05\alpha_h$	$0,90+0,10\alpha_h$
		$-1 \le \psi < 0$	$0,95+0,05\alpha_h(1+2\psi)$	$0,90-0,10\alpha_h(1+2\psi)$

Tab. 6.1: C_{my} according to table B.3 of EN 1993-1-1 [3]

In Tab. 6.2 some calculations performed by means of the above equivalent member method are opposed to the results of a FE-analysis and a calculation according to 2nd order theory. For three different systems calculation is done for three different values of transverse load or end moment each. With the different transverse load or end moment the quotient M/M_w is determined. In a second step the axial load N and the quotient N/N_w is determined. If the quotients N/N_w determined by the different methods are compared, a good agreement becomes apparent.

system	M/M_w	N/N_w calculated by			
		equivalent member method	2nd Order Theory	FE	
	0,20	0,46	0,46	0,45	$G=3N/mm^2$
	0,39	0,31	0,32	0,31	$E=6N/mm^2$
	0,79	0,10	0,10	0,10	$D=80mm$
	0,19	0,47	0,46	0,46	$t_F=0,6mm$
	0,39	0,33	0,32	0,33	$L=3500mm$
	0,78	0,12	0,10	0,11	$e_0=1/500 \cdot L$
	0,18	0,44	0,46	0,46	
	0,37	0,30	0,33	0,33	
	0,74	0,10	0,12	0,12	

Tab. 6.2: Comparison of different possibilities for design

7 Time-dependent behaviour

7.1 Basics

In addition to the deflection w_b due to bending, the deflection of a sandwich panel consists of the deflection w_v due to shear deformation resulting from transverse force (formula (2.5)).

Both, organic core materials such as polyurethane or expanded polystyrene and mineral wool show creep phenomena under long-term loads, e.g. dead-weight load and snow. If a constant load acts on a panel over a long period of time, the shear deformation of the core material and thus the shear deflection w_v increase. The shear strain γ increases with constant shear stress. For sandwich panels the time-dependent shear strain is usually described by a creep function $\varphi(t)$.

$$\gamma(t) = \gamma(0) \cdot \left(1 + \varphi(t)\right) \tag{7.1}$$

Therefore the time-dependent deflection is

$$w(t) = w_b + w_v(t) = w_b + w_v(0) \cdot \left(1 + \varphi(t)\right) \tag{7.2}$$

If the panels are loaded only by transverse forces creep effects can be considered by a reduction of the shear-modulus G_C. So for design we have a notional time-dependent shear-stiffness $GA(t)$.

$$w(t) = \frac{1}{B_S} \cdot \int M\overline{M}dx + \frac{1}{GA} \cdot \int V\overline{V}dx \cdot \left(1 + \varphi(t)\right) = \frac{1}{B_S} \cdot \int M\overline{M}dx + \frac{1}{GA(t)} \cdot \int V\overline{V}dx \tag{7.3}$$

$$GA(t) = \frac{G_C}{1 + \varphi(t)} \cdot A_C \tag{7.4}$$

To design sandwich panels, which are subjected to long-term loads, not the complete creep-function is necessary. Usually only two creep coefficients are used. The creep coefficient φ_{2000} is used to consider snow loads; the creep coefficient $\varphi_{100.000}$ is used to consider dead weight loads.

To determine the creep coefficients φ_t, the creep function $\varphi(t)$ is determined by (bending-) creep tests on panels subjected to a constant transverse (dead) load. In the test, the deflection of the panel is measured for a period of 1000 hours and the creep function is recalculated [1], [2].

$$\varphi(t) = \frac{w(t) - w(0)}{w(0) - w_b} \tag{7.5}$$

with

w(t)   deflection measured at time t

w(0)   initial deflection measured at time t=0

w_b bending deflection, determined by calculation

Based on the experimentally determined creep-function, both creep coefficients φ_{2000} and $\varphi_{100.000}$ are determined by extrapolation. For design purposes the creep coefficient φ_{2000} determined by testing is increased by 20%. So it is taken into account that a part of the creep deformation caused by snow loads during winter time is not recovered during summer time.

7.2   Creeping of axially loaded sandwich panels

Creeping of the core material results in an increase of the deflection of a panel. If, in addition to the transverse load, an axial load acts on the panel the increase of the deflection results also in an increase of the stress resultants moment and transverse force (Fig. 7.1). The normal stresses in the faces and the shear stress in the core also increase. Therefore, the long-term behaviour of the panels has not only to be considered in the design for serviceability limit state (deformation limit) but also in the design for ultimate limit state (load-bearing capacity), i.e. for the determination of the stress resultants.
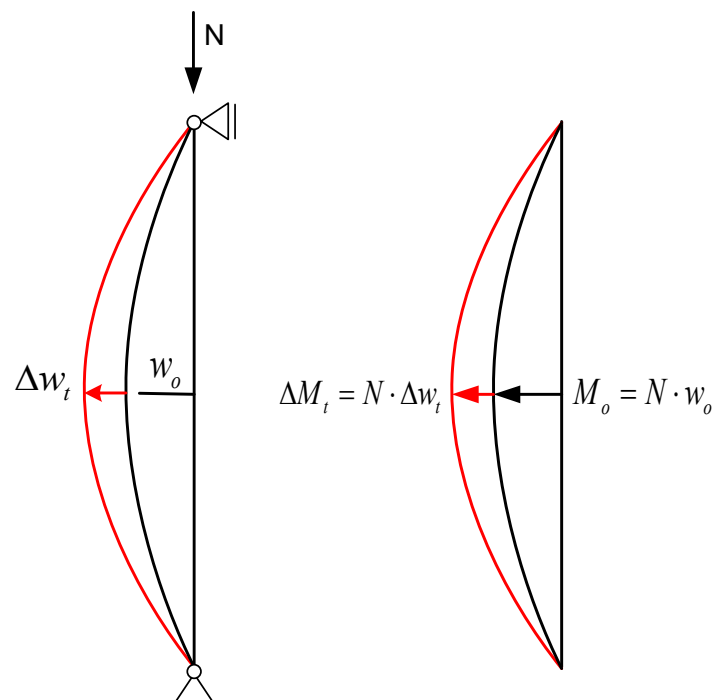

Fig. 7.1:   **Creeping of an axially loaded sandwich panel**

7.3   Long-term tests

To investigate the influence of axial loads on the creep behaviour of sandwich panels, long-term tests on axially loaded sandwich panels were performed. In creep tests, which are usually performed on panels with transverse load, the panels are loaded by a constant load and the time-dependent deflection is measured (Fig. 7.2).
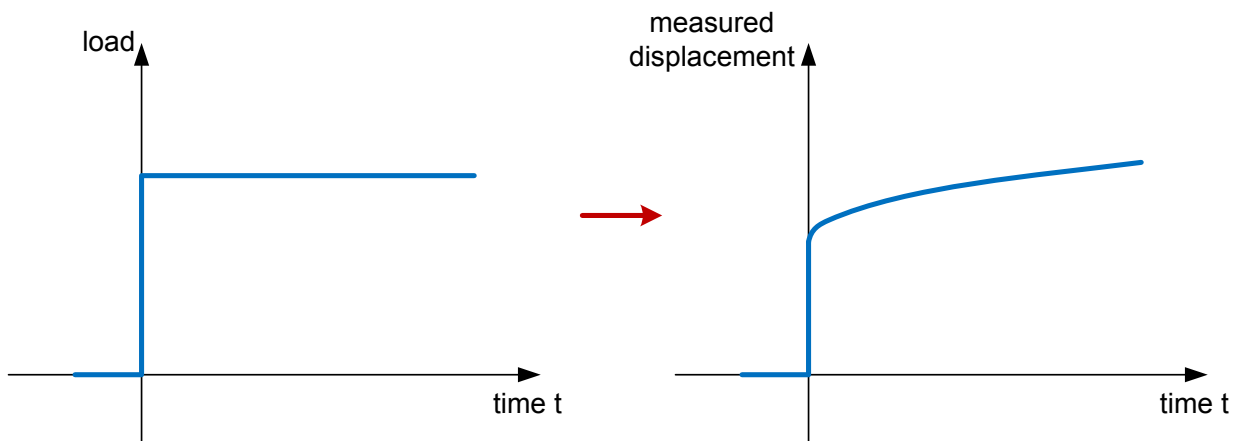
Fig. 7.2:   **Creep test**

To test panels with axial load this is an inapplicable procedure. So the long-term test with axial load were not performed as classical creep tests but as relaxation tests, i.e. a constant displacement is applied and a resulting time-dependent force or stress is measured (Fig. 7.3).
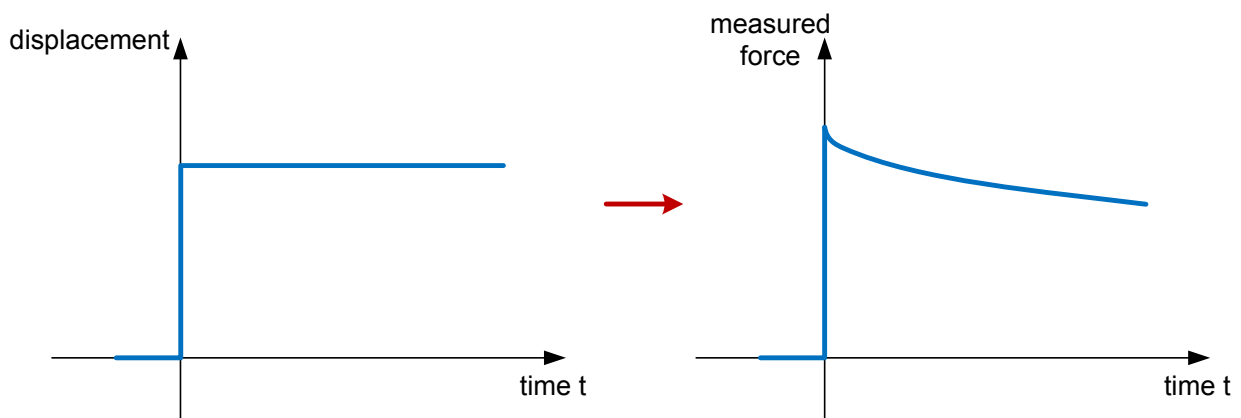

Fig. 7.3:   **Relaxation test**

During the long-term tests, the panels were loaded by an axial load corresponding to the working load to be expected in reality. For determination of the axial load it was assumed that wall panels are loaded by the loads applied from an overlying roof panel. For the roof panel a span of 6 m and a dead weight of about 0,12 kN/m^2 were assumed. With a snow load s_k = 0,68 kN/m^2 (snow load zone 2, 200 m above normal zero [4], [5]) an axial load of 2,4 kN/m ensues for the wall panels. This also approximates the indications in [9]. Here, an axial design load of 3,67 kN/m is assumed for the external wall of a building, which corresponds to a load of 2,6 kN/m for an averaged load factor of γ_F = (1,5+1,35)/2 = 1,425. The axial load in the tests was 2,8 kN/m (including test set-up).

Since the creep behaviour of different core materials differs from each other, panels with the common core materials (polyurethane, expanded polystyrene, mineral wool) were tested.
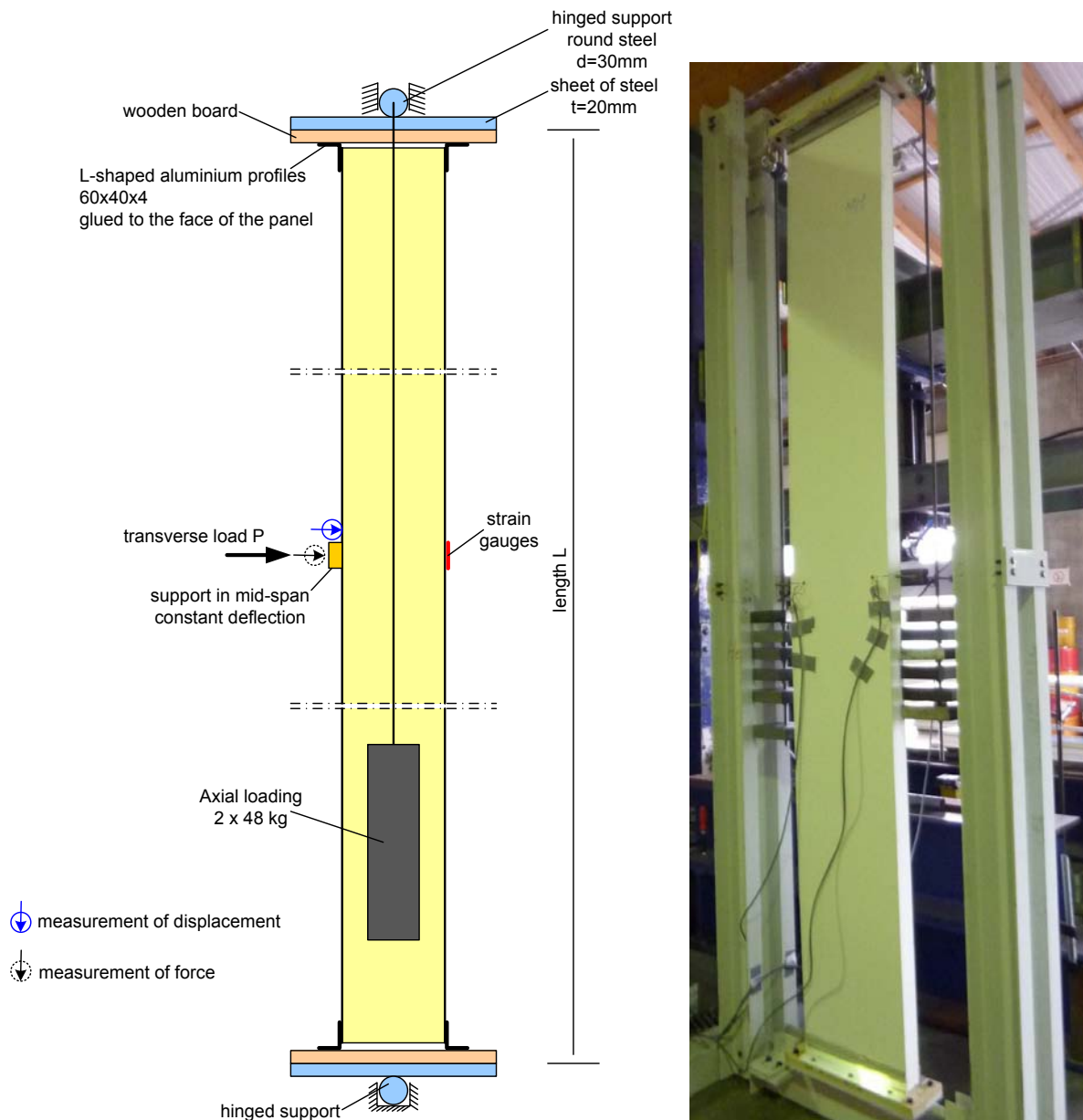
Fig. 7.4: Test set up for long-term tests on axially loaded sandwich panels

The test set-up for the long-term test is given in Fig. 7.4. To apply the axial load the same test set-up was used as in the buckling tests (section 4). Per type of panel two tests were performed. In the first test, the axial load was applied centrically, i.e. into both face sheets, in the second test the axial load was applied eccentrically only into one face sheet (Fig. 7.5).
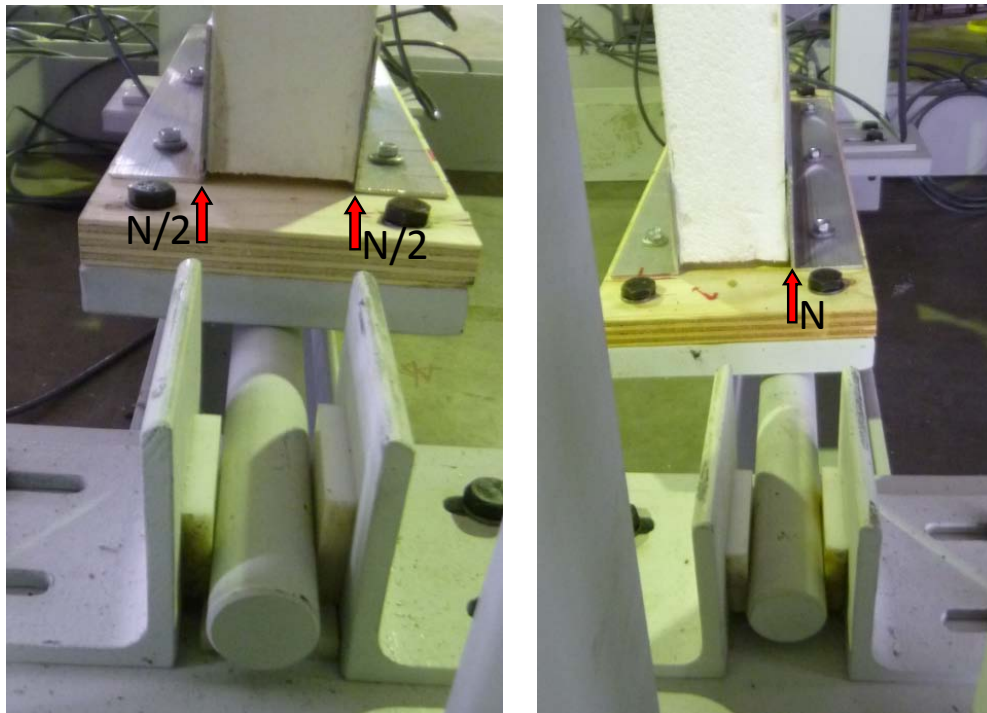
Fig. 7.5:   Centric and eccentric application of axial load

After applying the axial load, a deflection was applied to the panel via an additional support in mid-span (Fig. 7.6). The support was fixed and the deflection was kept constant over the test period.

Fig. 7.6:   Support at mid-span

The reaction force at the mid-support was continuously recorded during the test (Fig. 7.7). To measure the reaction force strain gauges were used which were applied on the thread rods, used to install the support (Fig. 7.7).
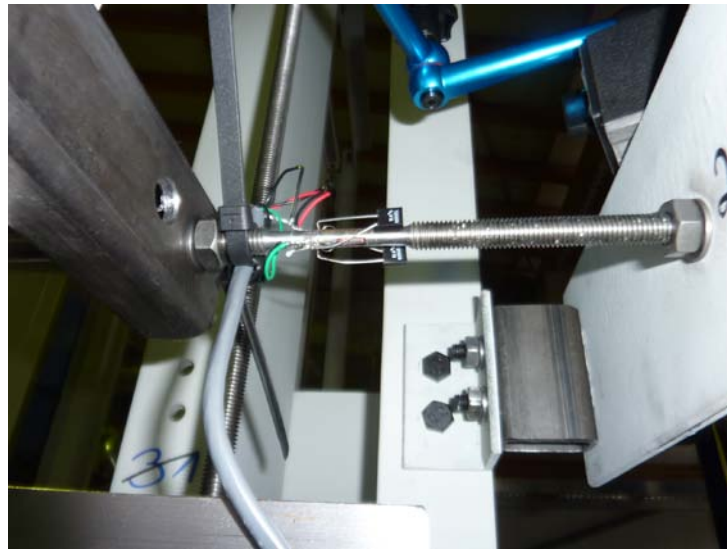
Fig. 7.7: Measurement of reaction forces at mid support (strain gauges)

In addition, in mid-span the strains in the face sheet subjected to tension were measured with strain gauges and also continuously recorded.

Fig. 7.8: Strain gauges at the face sheet subjected to tension

A compilation of the performed long-term tests is given in Tab. 7.1. A detailed documentation of the test results can be found in D3.2-part 4 [8].

No.	type of panel	face	core	application of axial load	initial deflection
F-1	F	steel, 0,75 mm	PU, 60 mm	centric	15,5 mm
F-2	F	steel, 0,75 mm	PU, 60 mm	eccentric	10,5 mm
G-1	G	steel, 0,60 mm	EPS, 60 mm	centric	15,5 mm
G-2	G	steel, 0,60 mm	EPS, 60 mm	eccentric	10,0 mm
H-1	H	GFRP, 1,8 mm	EPS, 60 mm	centric	15,5 mm
H-2	H	GFRP, 1,8 mm	EPS, 60 mm	eccentric	10,5 mm
I-1	I	steel, 0,60 mm	MW, 60 mm	centric	15,0 mm
I-2	I	steel, 0,60 mm	MW, 60 mm	eccentric	10,0 mm

Tab. 7.1: **Performed long-term tests**

For the purpose of comparison additionally to the long-term tests on axially loaded panels creep tests according to EN 14509 [1] were performed for each tested type of panel. The tests were performed on single-span panels which were subjected to a uniformly distributed dead load (Fig. 7.9, Tab. 7.2).
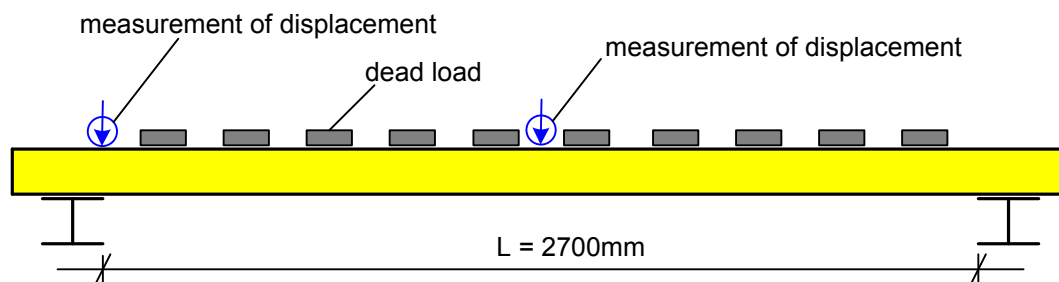

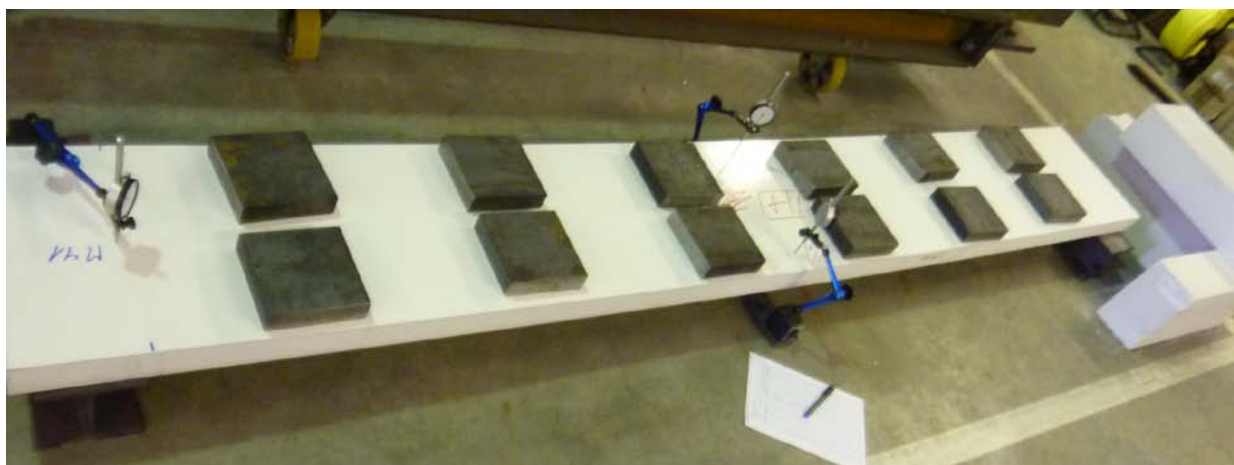**Fig. 7.9:** **Test set up for creep tests according to EN 14509**

Fig. 7.10: **Test set up for creep tests according to EN 14509**

No.	dead load
F	1,44 kN
G	1,44 kN
H	0,96 kN
I	0,64 kN

Tab. 7.2:   Dead load in creep tests

In addition the material properties of core and face layers were determined for each tested type of panel.

Also the results of the creep tests and the material properties are documented in D3.2-part 4 [8].

7.4   Evaluation of long-term tests

In the following it is verified that an axial force does not influence the creep behaviour of sandwich panels. So the creep coefficients determined according to EN 14509 by simple bending tests with transverse loading can also be used to design panels, which are axially loaded. Comparatively complex tests on axially loaded panels are not necessary.

For this purpose the reaction force P at mid support and the stresses in the face sheet are determined by calculation using the creep functions determined according to EN 14509 (bending creep tests). These calculated values are compared to the values determined in the tests on panels with axial load.

Based on the creep behaviour of the core material the reaction force P measured at mid-support decreases during the test (Fig. 7.11). For this reason, also the stresses and strains in the face sheets decrease.

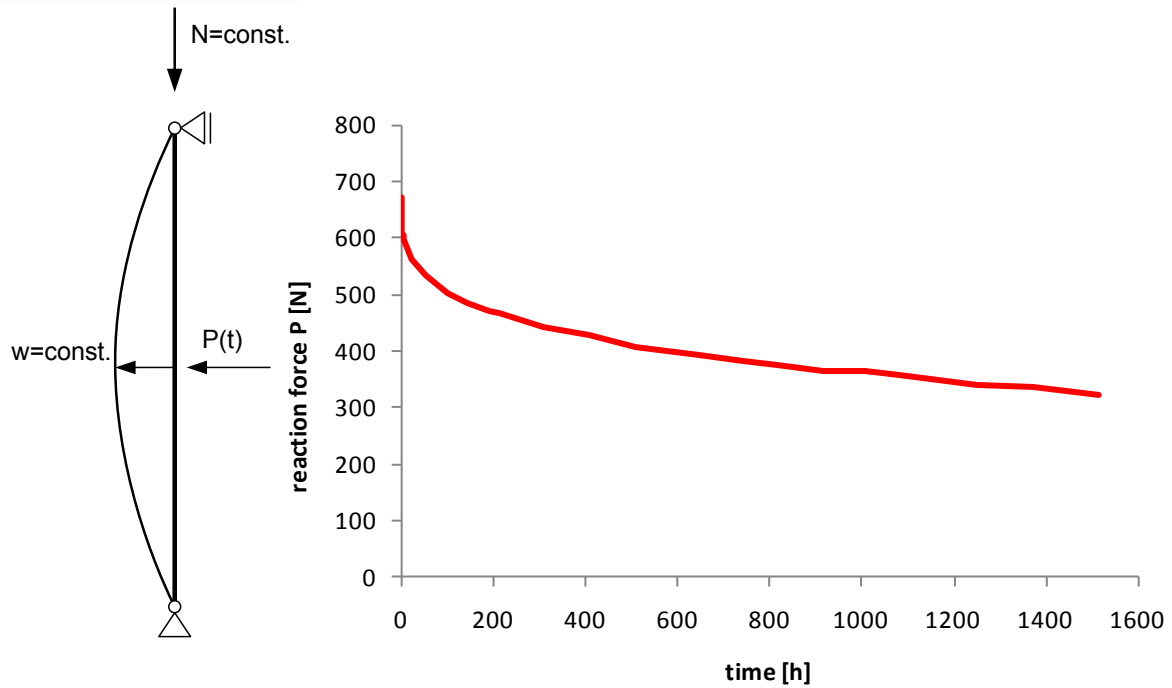**Fig. 7.11:** **Reaction force-time relationship for long-term tests**

At first, the creep function φ(t) was determined from the bending creep tests for each tested type of panel according to formula (7.5). For each type of panel (i.e. for each core material), the determined creep function φ(t) is presented in the following diagram.
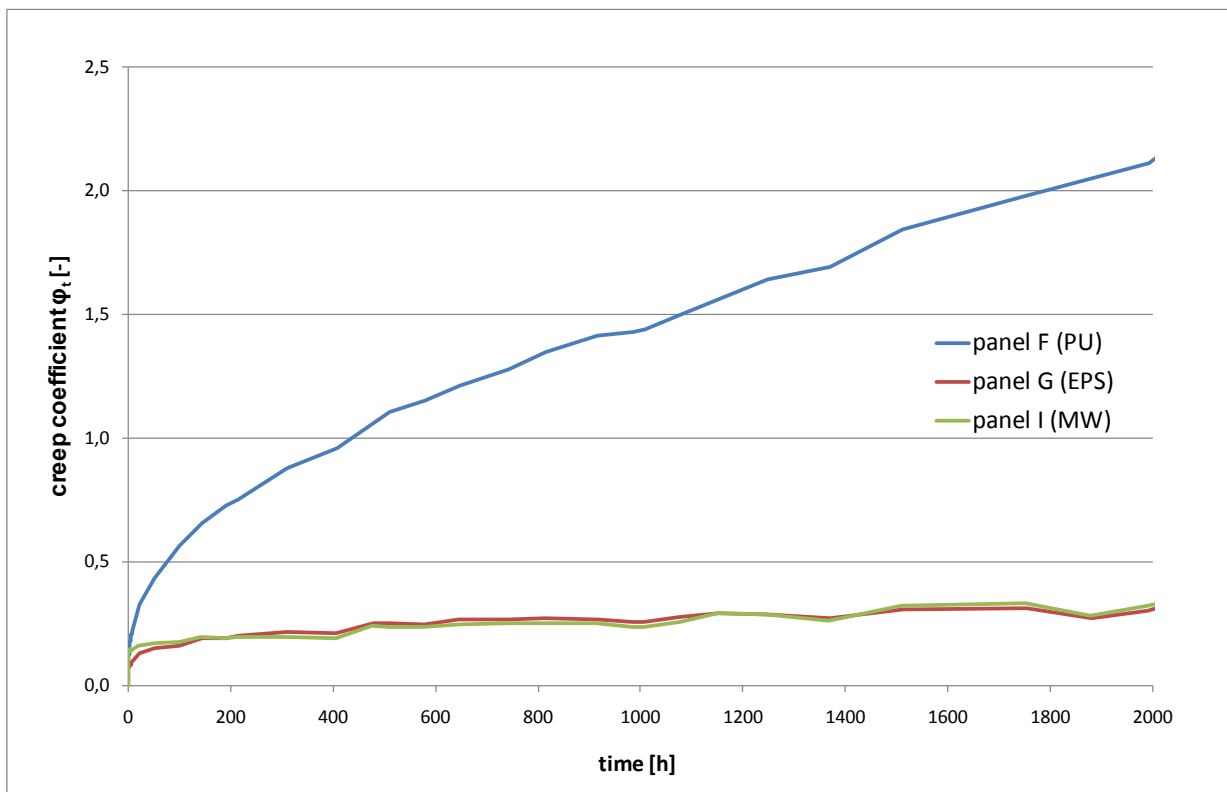

Fig. 7.12: **Creep functions**

The deflection w of a panel loaded both by an axial load N and by a concentrated load P in mid-span is calculated as follows

$$w = \left(\frac{P \cdot L^3}{48 \cdot B_S} + \frac{P \cdot L}{4 \cdot GA} + \frac{N \cdot e \cdot L^2}{8 \cdot B_S} \right) \cdot \alpha \tag{7.6}$$

with

e = 0   for centric axial load (tests -1)

e = D/2   for eccentric axial load (tests -2)

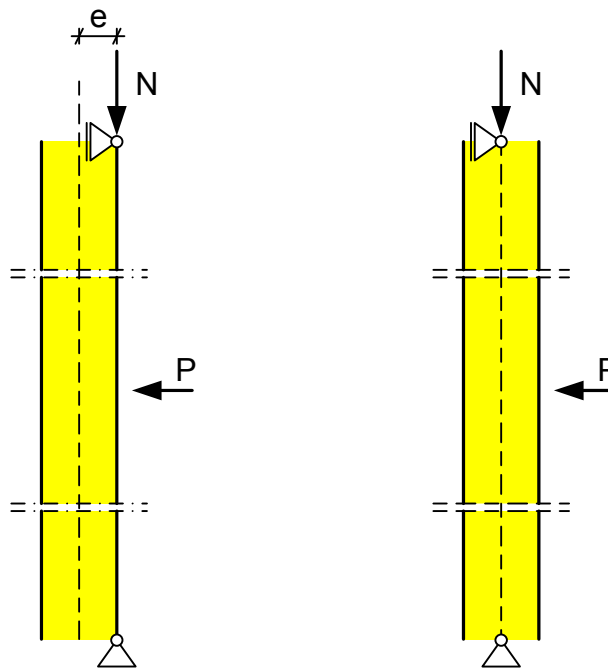α   amplification factor to consider effects of 2nd order theory

Fig. 7.13:   **Mechanical models for evaluation of long-term tests**

If creeping of the core material is considered by creep functions φ(t), constant loads P and N result in the time dependent deflection w(t).

$$w(t) = \left[\left(\frac{P \cdot L^3}{48 \cdot B_S} \right) + \left(\frac{P \cdot L}{4 \cdot GA} \right) \cdot \left(1 + \varphi(t) \right) + \left(\frac{N \cdot e \cdot L^2}{8 \cdot B_S} \right) \right] \cdot \alpha \tag{7.7}$$

In the tests the deflection w is kept constant. Also the axial load N is constant. So the reaction force P at mid-support depends on the time and decreases due to the creep behaviour of the core material. Considering the axial force N, the constant deflection w_0 and the creep function φ(t), the reaction force P(t) can be determined according to the following equation.

$$P(t) = \frac{\dfrac{w_0}{\alpha} - \dfrac{N \cdot e \cdot L^2}{8 \cdot B_S}}{\dfrac{L^3}{48 \cdot B_S} + \dfrac{L}{4 \cdot GA} \cdot \left(1 + \varphi(t)\right)} \tag{7.8}$$

Caused by the time dependence of the force P also the stresses in the face sheets depend on the time. The normal stress $\sigma_F(t)$ in the face sheet subjected to tension is calculated as follows

$$\sigma_F(t) = \frac{P(t) \cdot L}{4 \cdot D \cdot A_F} + \frac{N \cdot w_0}{D \cdot A_F} + \frac{N \cdot e}{D \cdot A_F} - \frac{N}{2 \cdot A_F} \tag{7.9}$$

With the creep functions $\varphi(t)$ determined from the bending creep tests on panels with transverse load (Fig. 7.12), the time-dependent reaction force P(t) at mid-support and from this, the time-dependent stress $\sigma_F(t)$ in the face sheet were determined using the above equations.
In the following diagrams (Fig. 7.14 to Fig. 7.19), the forces and stresses determined in the tests are opposed to calculated values. The measured values were standardized to the calculated value at about t = 150 h.

Fig. 7.14: **Long-term test F-1**

panel F (PU), eccentric loading
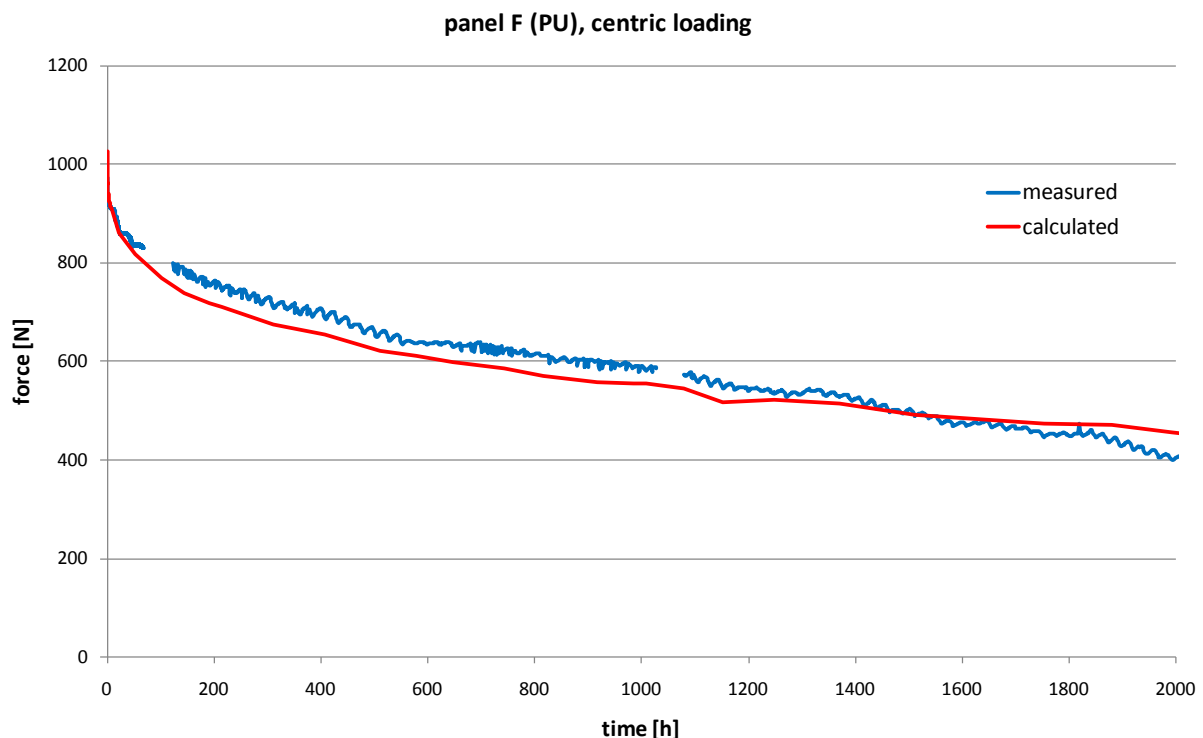
Fig. 7.15:   Long-term test F-2
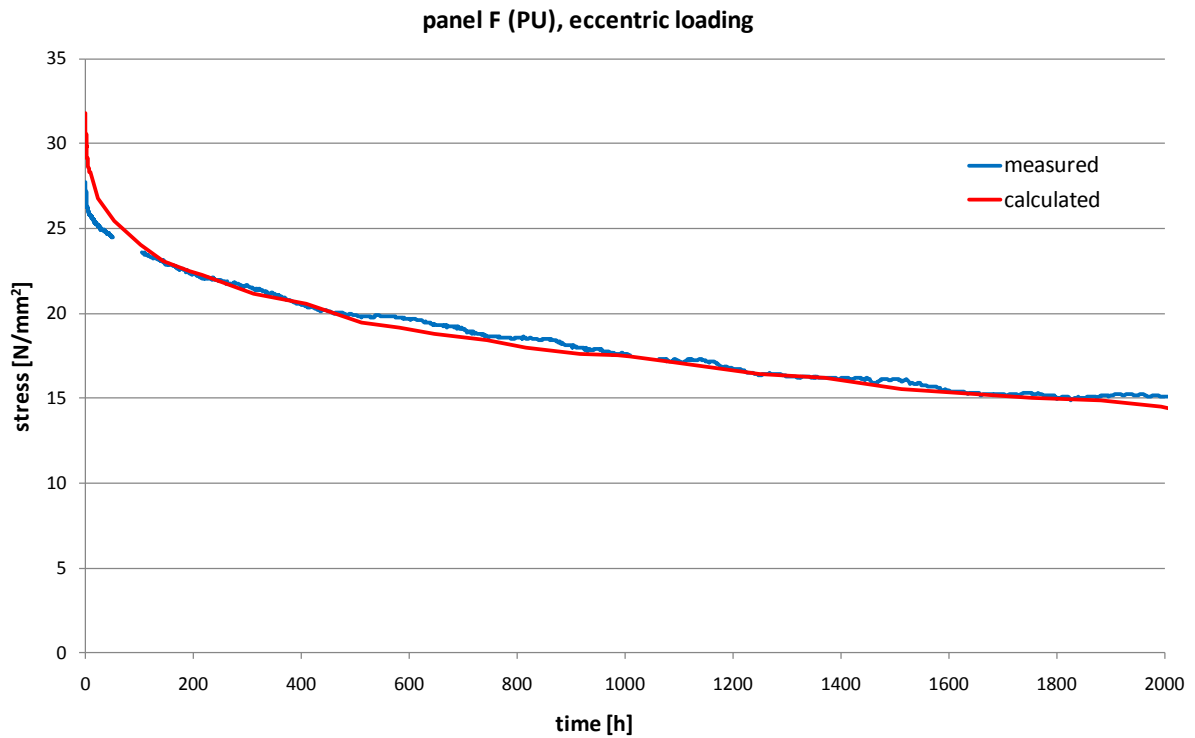
panel G (EPS), centric loading
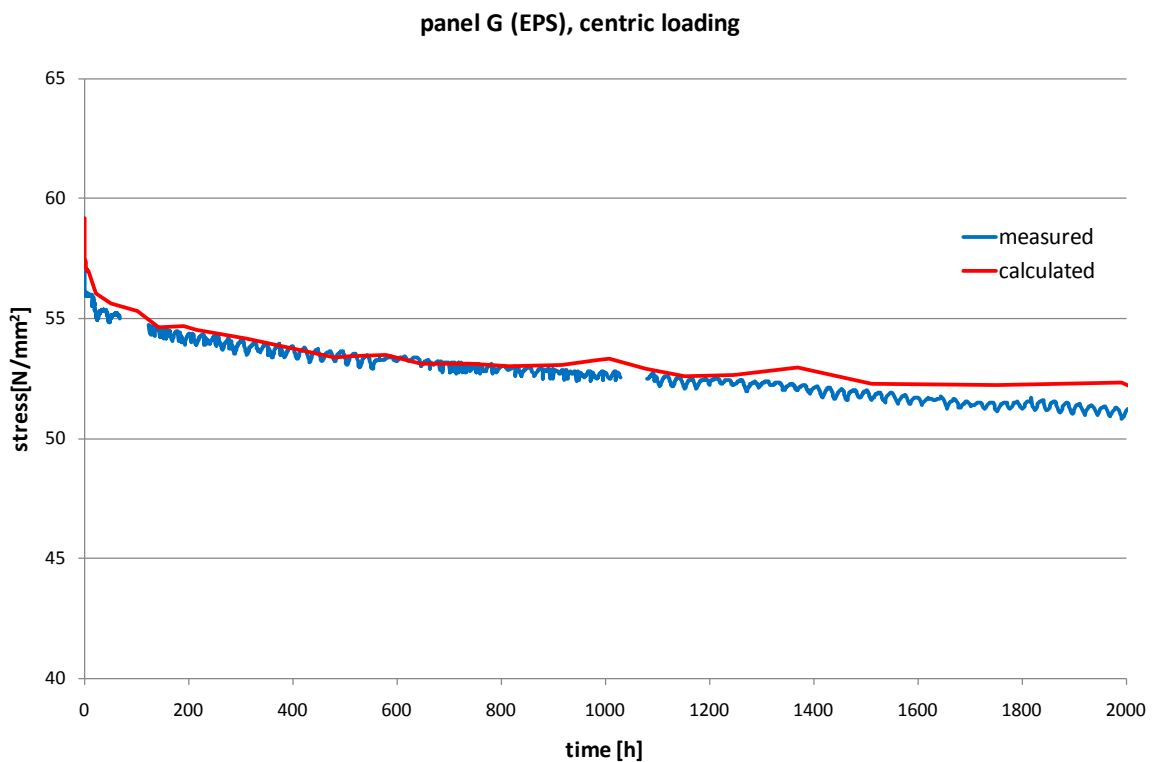

Fig. 7.16:   Long-term test G-1

panel G (EPS), eccentric loading
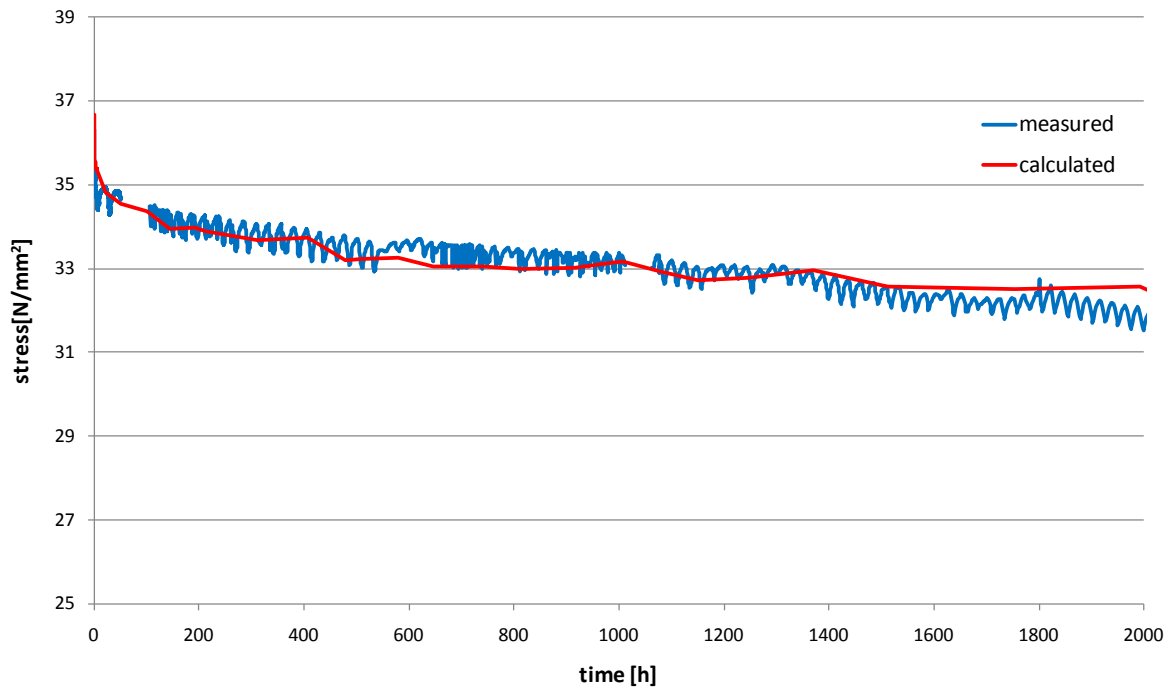
Fig. 7.17:   **Long-term test G-2**

panel I (MW), centric loading

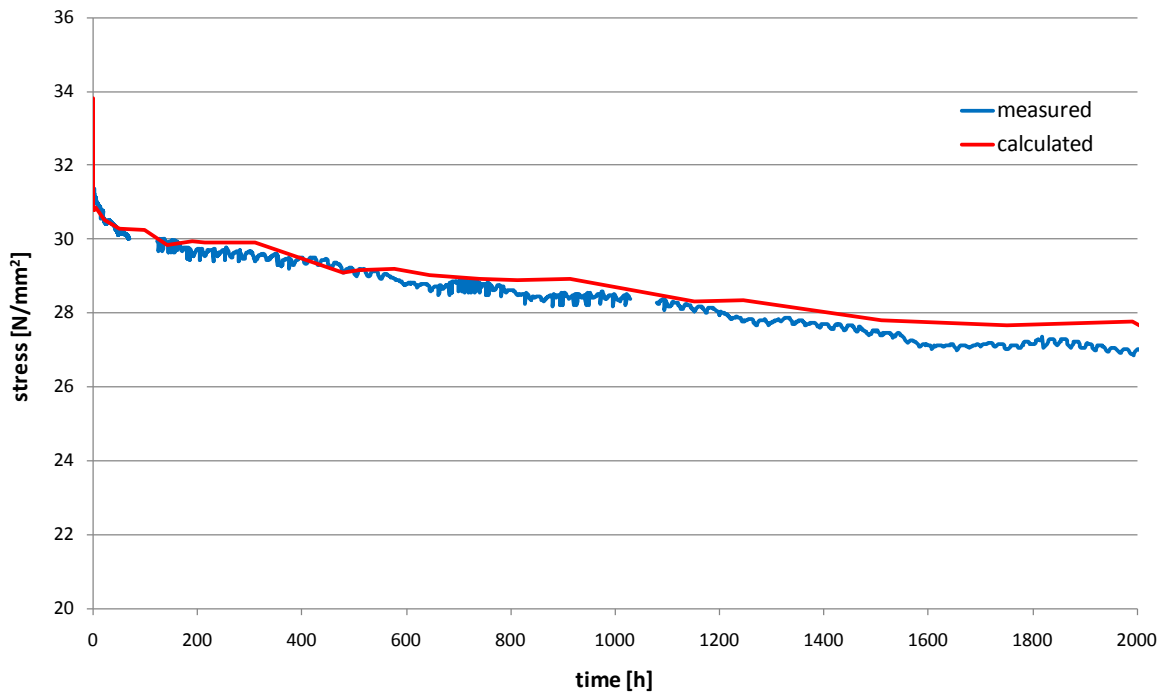**Fig. 7.18:**   **Long-term test I-1**
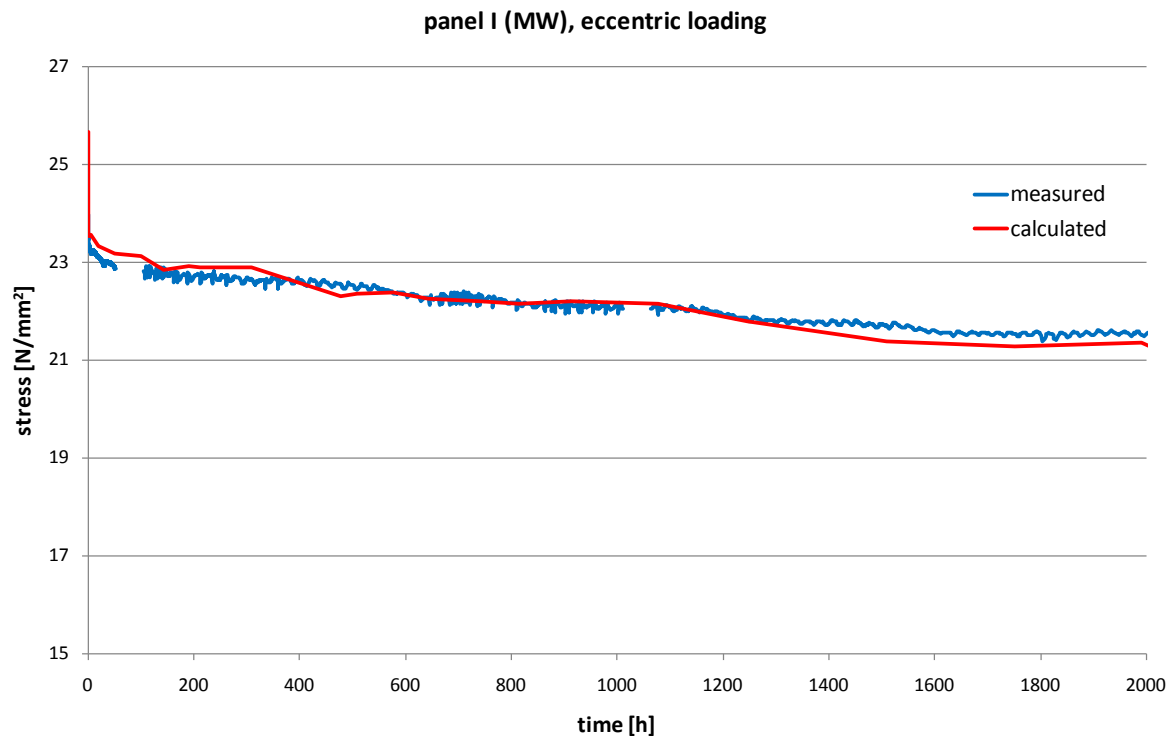
panel I (MW), eccentric loading

Fig. 7.19: **Long-term test I-2**

Based on the good agreement between the scopes of analytically and experimentally deter-
mined curves, a relevant influence of an axial force on the creep behaviour of the sandwich
panels can be excluded. Therefore, the creep coefficients used for the design of panels sub-
jected to transverse loads can also be used for the design of axially loaded panels. This pro-
cedure has the advantage that all required coefficients can be determined in simply performed
creep tests according to EN 14509 and no extensive long-term tests with axial loads must be
carried out. Furthermore, for many panels the required parameters are already known.

7.5   Consideration of long-term effects in design formulae

When designing sandwich panels, creep effects must be considered for long-term acting
loads such as dead weight and snow. According to EN 14509 this is done by an increase of
the shear deflection w_v using creep coefficients $\varphi_t.$ The same procedure can be applied for the
design of panels with axial load or combined load. The additional axial load as well as effects
of 2nd order theory must be considered in the corresponding formulae. Furthermore it has to
be noted, that not only the deflection, but also the stress resultants moment and transverse
force increase, if the panel is loaded by long-term loads.

We assume a panel, which is loaded by a short-term load as well as by a long-term load. The
shear part $w_{lt,v}$ of the deflection caused by the long-term load increases due to creep effects.
In addition the entire deflection according to 1st order theory increases due to effects of 2nd

order theory. This is considered by the amplification factor α. So the deflection w_t has to be calculated as follows

$$w_t = \left(w_{st,b} + w_{st,v} + w_{lt,b} + w_{lt,v} \cdot (1+\varphi_t)\right) \cdot \alpha \tag{7.10}$$

with

deflection due to short-term loads, e.g. wind:

$$w_{st} = w_{st,b} + w_{st,v} \tag{7.11}$$

deflection due to long-term load, e.g. snow or self-weight:

$$w_{lt} = w_{lt,b} + w_{lt,v} \tag{7.12}$$

α amplification factor (2nd order theory)

An increase of deflections also results in an increase of the stress resultants moment and transverse force if an axial load exists. This means that besides effects from the 2nd order theory also creep effects must be considered for determination of bending moment and transverse force. In this case it is useful not to work with the creep coefficients φ_t describing the increase of the shear deformation, but with a "sandwich creep coefficient" φ_{St} describing the increase of the deformation of the sandwich part of the cross-section [18].

$$w_t = w_{st} + w_{lt} \cdot (1+\varphi_{St}) \tag{7.13}$$

with

$$\varphi_{St} = \frac{k}{1+k} \cdot \varphi_t \tag{7.14}$$

$$k = \frac{w_v}{w_b} = \frac{B_S}{GA} \cdot \frac{\int V\overline{V}dx}{\int M\overline{M}dx} \tag{7.15}$$

The "sandwich factor" k corresponds to the relationship between deflection due to shear deformation and deflection due to bending. Unlike the creep coefficient φ_t the "sandwich creep coefficient" φ_{St} is not a material parameter. It also considers the loads acting on the panel. Therefore it has to be calculated for each single load case.

The moment caused by long-term loads has to be increased by the coefficient φ_{St}. As well the moment due to short-term load as the moment due to long-term load have to be amplified according to 2nd order effects. The time-dependent bending moment can be calculated in the following way

$$M_t = \left(M_{st} + M_{lt} \cdot (1+\varphi_{St})\right) \cdot \alpha \tag{7.16}$$

with

M_{st} moment due to short-term loads

M_{lt} moment due to long term loads

Depending on the load, the creep coefficient corresponding to the duration of the load effect has to be applied. As long-term acting loads usually dead weight and snow are available. According to [1] and [2], for snow, duration of load effect of 2.000 h is stipulated, for dead weight of 100.000 h. So for design the creep coefficient φ_{2000} is used for snow loads, $\varphi_{100.000}$ for dead weight loads. For a panel loaded by self-weight, snow and wind the deflection can be calculated with the following formula.

$$w_t = \left(w_{W,b} + w_{W,v} + w_{S,b} + w_{S,v} \cdot (1 + \varphi_{2000}) + w_{G,b} + w_{G,v} \cdot (1 + \varphi_{100000}) \right) \cdot \alpha \tag{7.17}$$

with

deflection due to wind load:

$$w_W = w_{W,b} + w_{W,v} \tag{7.18}$$

deflection due to snow load:

$$w_S = w_{S,b} + w_{S,v} \tag{7.19}$$

deflection due to self-weight load:

$$w_G = w_{G,b} + w_{G,v} \tag{7.20}$$

α amplification factor for effects of 2nd order theory

φ_{2000} creep coefficient for snow loads (2000 h)

$\varphi_{100.000}$ creep coefficient for self-weight loads (100.000 h)

The bending moment of a panel subjected to wind, snow and self-weight load is calculated in the following way

$$M_t = \left(M_W + M_S \cdot (1 + \varphi_{S2000}) + M_G (1 + \varphi_{S100000}) \right) \cdot \alpha \tag{7.21}$$

with

M_W moment due to wind load:

M_S moment due to snow load

M_G moment due to self-weight load

φ_{S2000} coefficient for snow loads (2000 h)

$\varphi_{S100.000}$ coefficient for self-weight loads (100.000 h)

7.6 Typical loads on wall panels of frameless structures

In Fig. 7.20 wall panels of frameless structures with typical loads and an imperfection e_0 are presented.
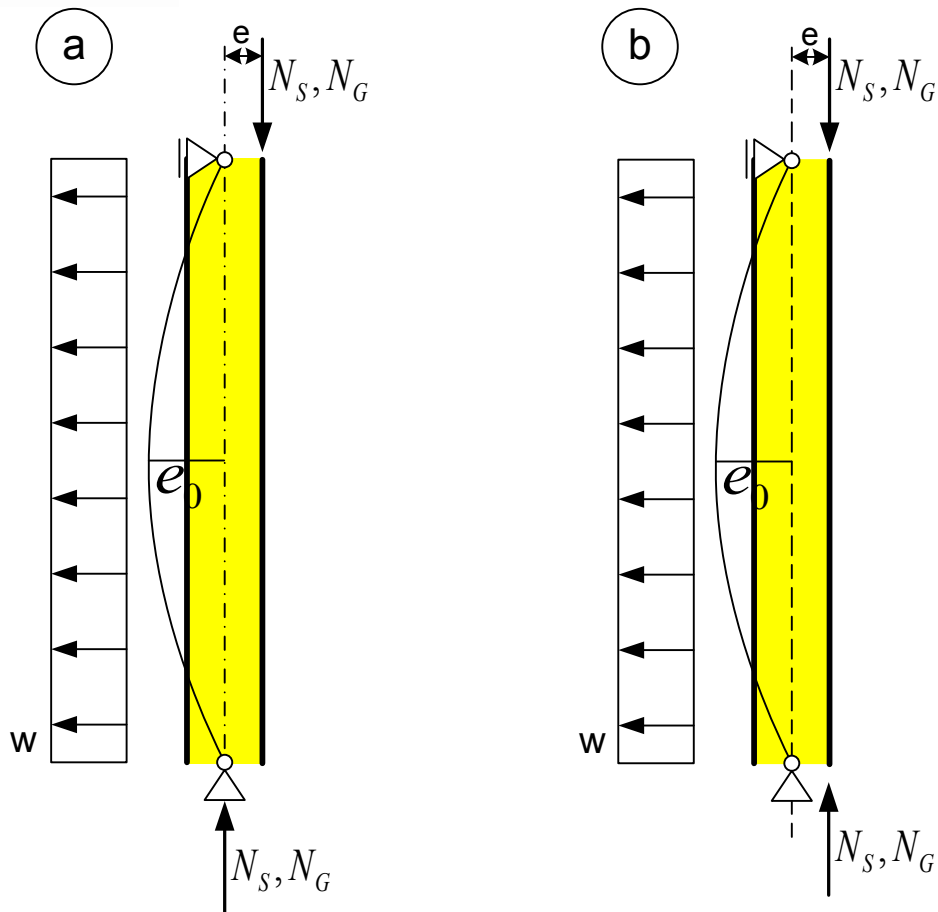
Fig. 7.20: **Wall panels with typical loads**

The normal force N usually arises out of superimposed loads from snow and dead weight of the overlying ceiling. So the axial loads N are long-term loads. Axial loads are mostly applied to only one face sheet of the wall panel. So fixed-end moments M^N arise, which are also long-term loads (Fig. 7.21).

$$M^N = N \cdot e \tag{7.22}$$

with

e   distance from loaded face to centroidal axis of the of panel, usually $e = \dfrac{D}{2}$

Fig. 7.21: **End moment M^N at the upper end**

Depending on the construction an end moment M^N can also act on the lower end of the panel.
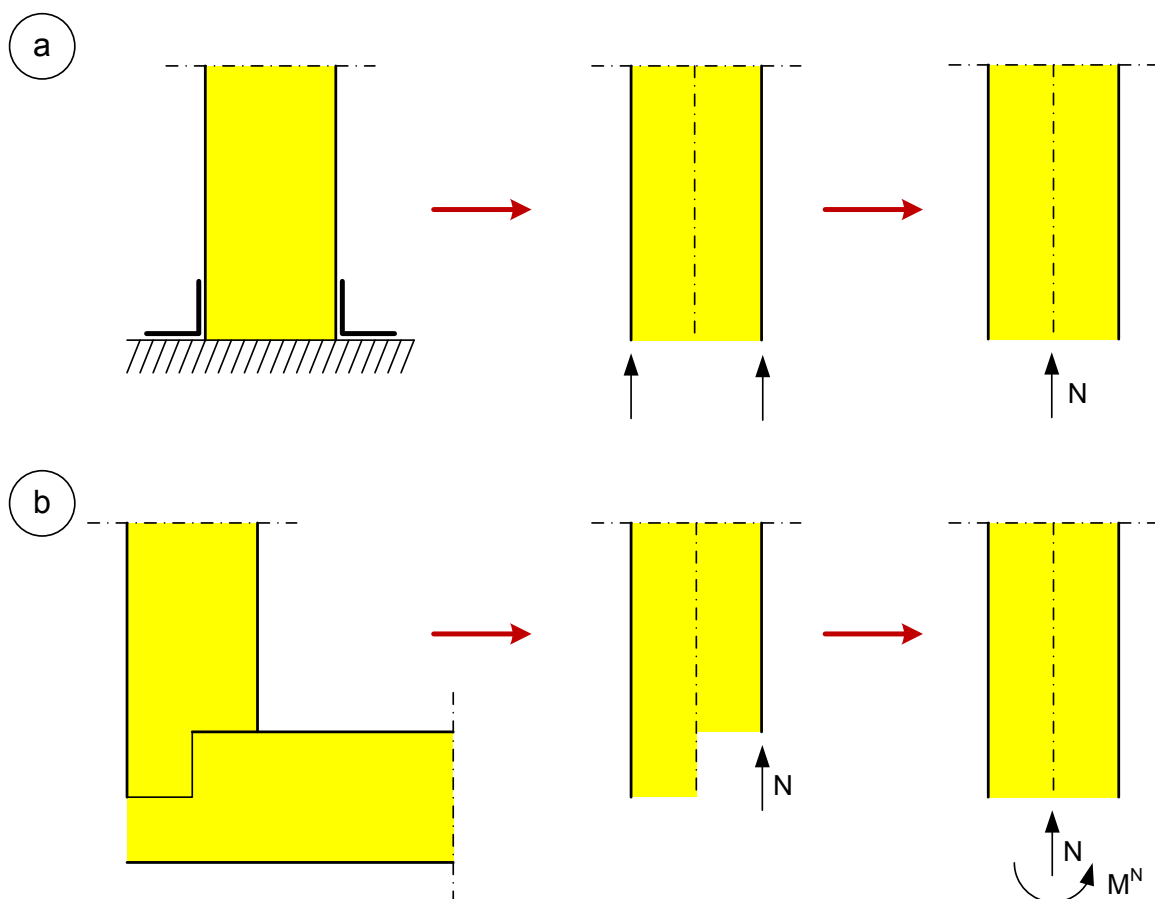
Fig. 7.22: **End moment M^N at the lower end**

Due to long-term axial loads, also geometrical imperfections e_0 result in long-term moments and transverse forces. A geometrical imperfection e_0 can be considered by application of a constant equivalent line load q_{e0} [3].
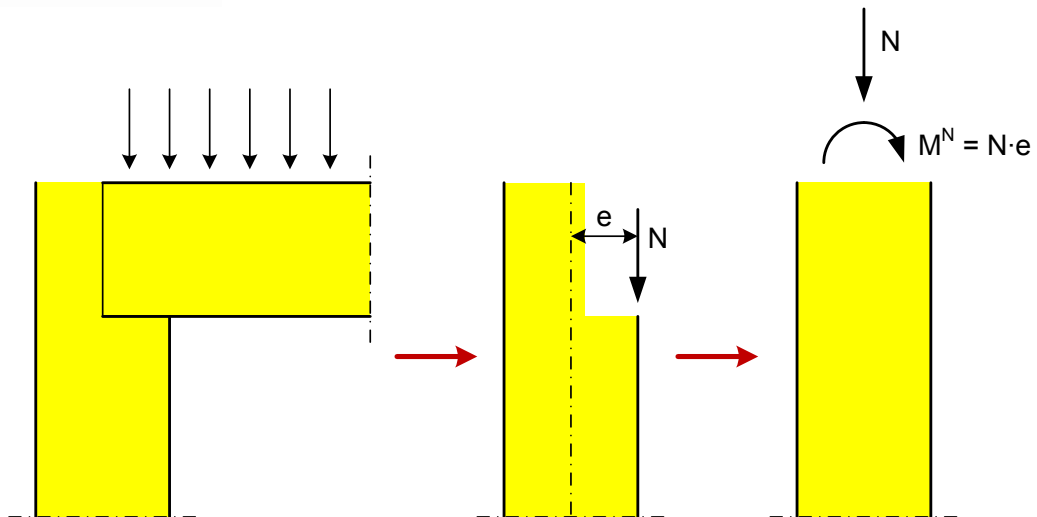
$$q_{e0} = N \cdot 8 \cdot \frac{e_0}{L^2} \qquad (7.23)$$

Analogous to the geometrical imperfection, also a deflection w_T from temperature differences between internal face and external face can be considered by an equivalent line load q_{wT}.

$$q_{wT} = N \cdot 8 \cdot \frac{w_T}{L^2} = N \cdot \Delta T \cdot \frac{\alpha_F}{D} \qquad (7.24)$$

In Fig. 7.23 the considered panels and the corresponding loads are shown.
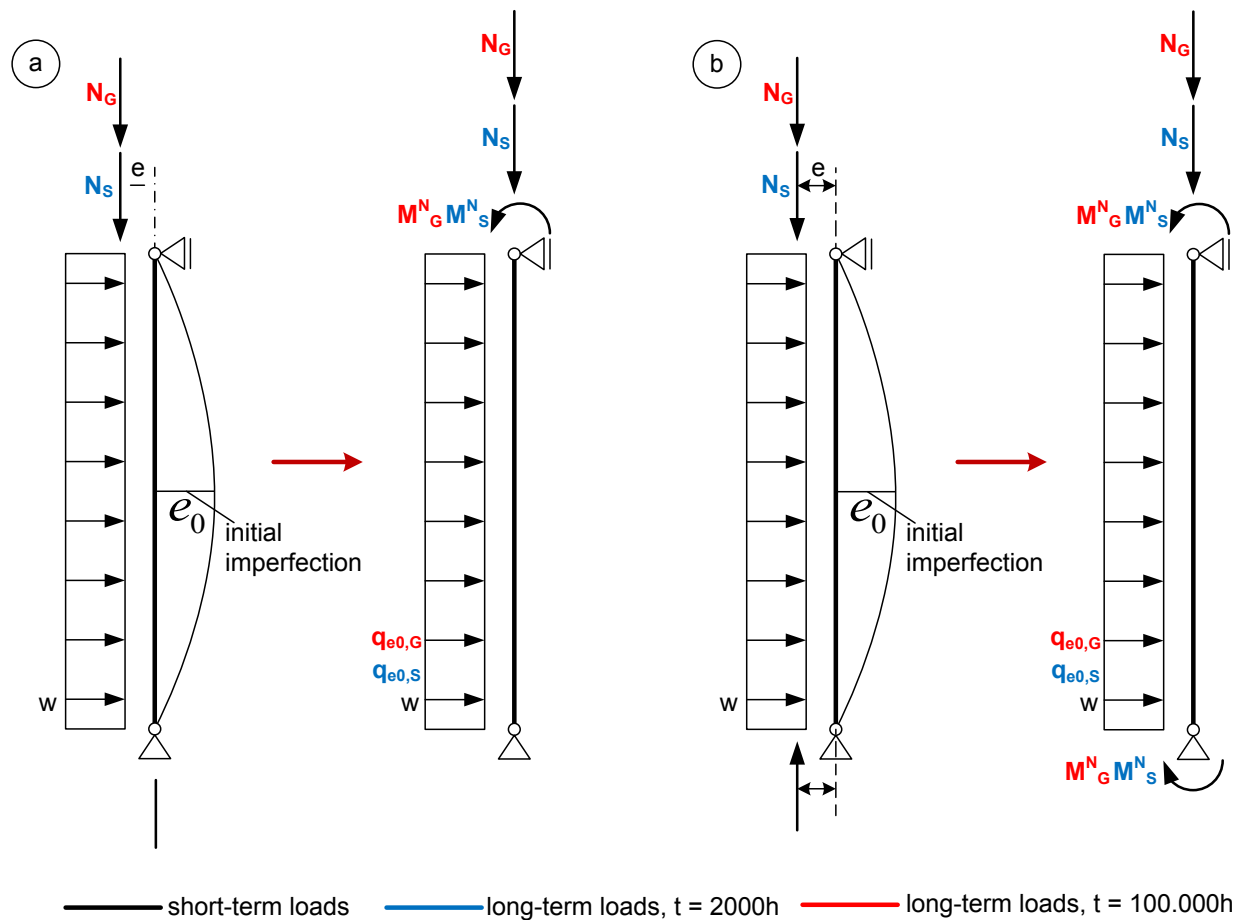
Fig. 7.23: **Loads acting on the wall panel**

For wall panels with the loading given above, the distribution of moment and transverse force is given in Fig. 7.24 (1st order theory, without consideration of creep effects).

Transverse load / Axial force and global imperfection / end moment (a) / end moment (b)

Load

Bending moment

$\dfrac{w \cdot L^2}{8}$, $N \cdot e_0$, $\dfrac{1}{2} M^N$, M^N

$M^N = N \cdot e$

Transverse force

$\dfrac{w \cdot L}{2}$, $\dfrac{N \cdot 4 \cdot e_0}{L}$, $\dfrac{M^N}{L}$, 0

Fig. 7.24: **Distribution of moment and transverse force**

So the bending and shear deflection is

a)

$$w_b = \frac{1}{B_S} \cdot \left(\frac{5}{384} \cdot w \cdot L^4 + \frac{40}{384} \cdot N \cdot e_0 \cdot L^2 + \frac{1}{16} \cdot N \cdot e \cdot L^2 \right) \qquad (7.25)$$

$$w_v = \frac{1}{GA} \cdot \left(\frac{w \cdot L^2}{8} + N \cdot e_0 + 0 \right) \qquad (7.26)$$

b)

$$w_b = \frac{1}{B_S} \cdot \left(\frac{5}{384} \cdot w \cdot L^4 + \frac{40}{384} \cdot N \cdot e_0 \cdot L^2 + \frac{1}{8} \cdot N \cdot e \cdot L^2 \right) \tag{7.27}$$

$$w_v = \frac{1}{GA} \cdot \left(\frac{w \cdot L^2}{8} + N \cdot e_0 + 0 \right) \tag{7.28}$$
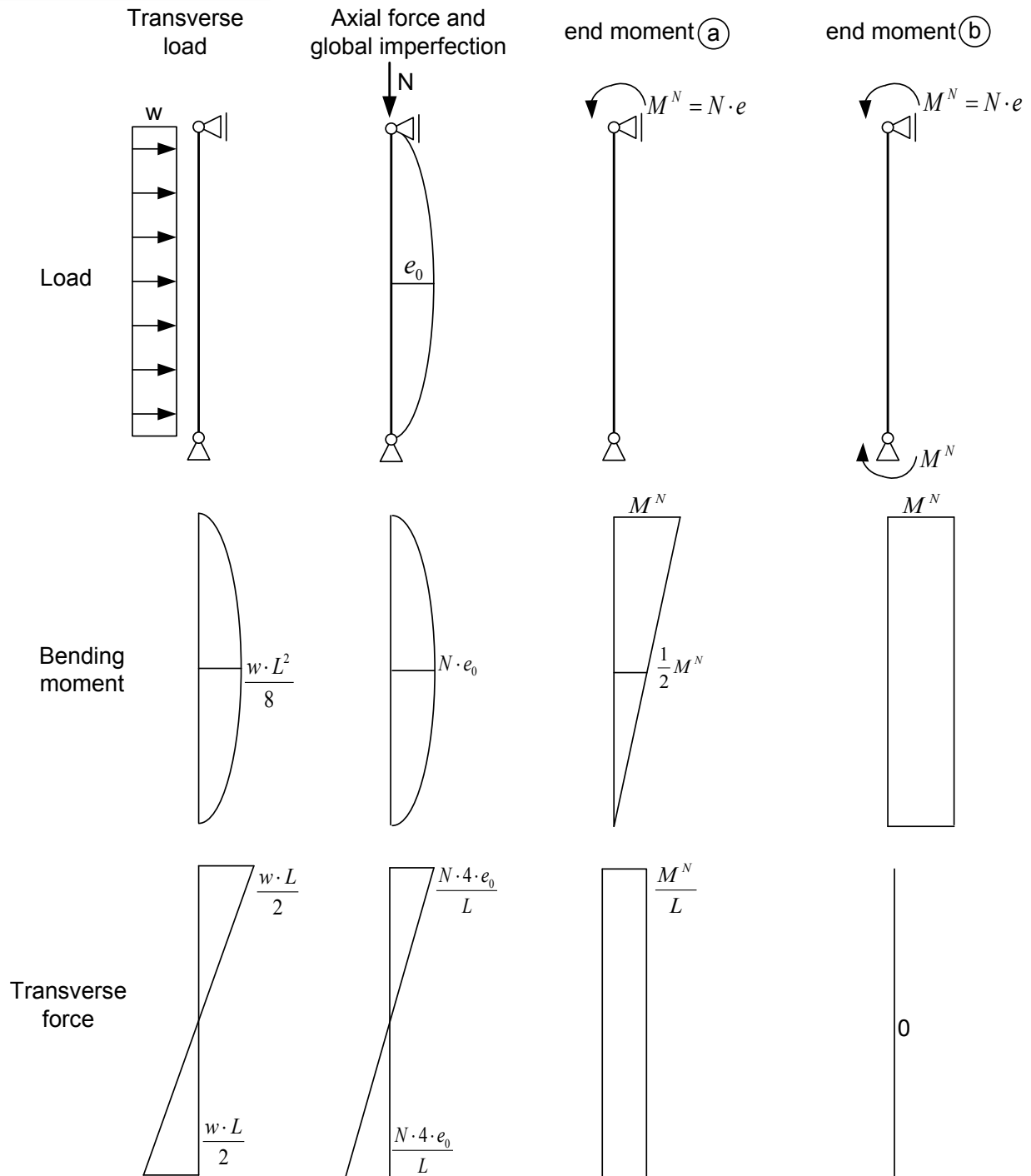
Remark:

To determine the transverse force resulting from a global imperfection e_0 and an axial load N a constant equivalent line load is assumed, which also results in the bending moment $N \cdot e_0$.

$$\frac{q_{e0} \cdot L^2}{8} = N \cdot e_0 \tag{7.29}$$

$$q_{e0} = N \cdot 8 \cdot \frac{e_0}{L^2} \tag{7.30}$$

The deflection caused by this load is

$$w_b = \frac{5}{384} \cdot \frac{q_{e0} \cdot L^4}{B_S} = \frac{40}{384} \cdot \frac{N \cdot e_0 \cdot L^2}{B_S} \tag{7.31}$$

$$w_v = \frac{q_{e0} \cdot L^2}{8 \cdot GA} = N \cdot e_0 \tag{7.32}$$

To calculate the factor k only long-term loads are considered.

a)

$$w_{lt,b} = \frac{1}{B_S} \cdot \left(\frac{40}{384} \cdot N \cdot e_0 \cdot L^2 + \frac{1}{16} \cdot N \cdot e \cdot L^2 \right) \tag{7.33}$$

$$w_{lt,v} = \frac{1}{GA} \cdot \left(N \cdot e_0 \right) \tag{7.34}$$

b)

$$w_b = \frac{1}{B_S} \cdot \left(\frac{40}{384} \cdot N \cdot e_0 \cdot L^2 + \frac{1}{8} \cdot N \cdot e \cdot L^2 \right) \tag{7.35}$$

$$w_v = \frac{1}{GA} \cdot \left(N \cdot e_0 \right) \tag{7.36}$$

So the "sandwich factor" k which is needed to consider long-term effects results for the above wall panels in

a)

$$k = \frac{w_{lt,v}}{w_{lt,b}} = \frac{B_S}{GA} \cdot \frac{N \cdot e_0}{\frac{1}{16} \cdot N \cdot e \cdot L^2 + \frac{40}{384} \cdot N \cdot e_0 \cdot L^2} = \frac{B_S}{GA \cdot L^2} \cdot \frac{e_0}{\frac{1}{16} \cdot e + \frac{40}{384} \cdot e_0} \qquad (7.37)$$

$$k = \frac{B_S}{GA \cdot L^2} \cdot \frac{48 \cdot e_0}{3 \cdot e + 5 \cdot e_0} \qquad (7.38)$$

b)

$$k = \frac{w_{lt,v}}{w_{lt,b}} = \frac{B_S}{GA} \cdot \frac{N \cdot e_0}{\frac{1}{8} \cdot N \cdot e \cdot L^2 + \frac{40}{384} \cdot N \cdot e_0 \cdot L^2} = \frac{B_S}{GA \cdot L^2} \cdot \frac{e_0}{\frac{1}{8} \cdot e + \frac{40}{384} \cdot e_0} \qquad (7.39)$$

$$k = \frac{B_S}{GA \cdot L^2} \cdot \frac{48 \cdot e_0}{6 \cdot e + 5 \cdot e_0} \qquad (7.40)$$

8 Partial safety factors

To design a sandwich panel according to EN 14509 [1] design calculations for the serviceability limit state and for the ultimate limit state are done. For axially loaded sandwich panels as given above this results in the following procedure:

<u>Serviceability limit state</u>

- Limitation of deflection

$$w \le w_{max} \qquad (8.1)$$

According to EN 14509 for wall panels

$$w_{ult} = \frac{L}{100} \qquad (8.2)$$

can be used, if there are not any other values from national standards.

The loads have to be determined using the load factors γ_F and combination coefficients ψ for serviceability limit state.

<u>Ultimate limit state</u>

- Wrinkling of a face sheet

$$\sigma_{F,d} \le \sigma_{w,d} \qquad (8.3)$$

- Shear failure of the core

$$\tau_{C,d} \le f_{Cv,d} \qquad (8.4)$$

The loads, which are used to calculate the normal stress $\sigma_{F,d}$ in the face and the shear stress $\tau_{C,d}$ in the core, have to be determined using the load factors γ_F and combination coefficients ψ for ultimate limit state.

The resistance values of wrinkling stress $\sigma_{w,d}$ of the face and shear strength $f_{Cv,d}$ of the core material have to be calculated by dividing the characteristic values by the material factor γ_M.

$$\sigma_{w,d} = \frac{\sigma_{w,k}}{\gamma_M} \qquad (8.5)$$

$$f_{Cv,d} = \frac{f_{Cv,k}}{\gamma_M} \qquad (8.6)$$

The characteristic values $\sigma_{w,k}$ and $f_{Cv,k}$ are determined by testing. Usually they can be found on the CE-mark of the panel. For sandwich panels the material factors γ_M represent the variability of the mechanical properties of the sandwich panel. They are determined by the results of initial type testing and factory production control.

The load factors γ_F are given by national specifications. They can be found in EN 1990 [6] and the related national annex.

9 Summary

In addition to the usual application as space enclosing components, in small buildings sandwich panels are partly also used without supporting substructure. This results in the question of the load-bearing capacity of the panels that are now, in addition to transverse loads, also subjected to axial loads. Using FE-analyses and tests, it could be shown that the panels subjected to axial loads can be designed according to the 2nd order theory with the amplification factor α. The wrinkling stress determined in simple bending tests can be used as ultimate stress. In the presented design method, also the long-term behaviour of the panels, i.e. creeping of the core material, can be considered. Only the creep coefficients, which are also used for the design of panels subjected to transverse loads, have to be known.

Using the design model presented above there is no necessarily of any additional test to design axially loaded sandwich panels. Only the parameters used for the design of panels subjected to transverse loads have to be known.

In the annexes of the report a summary of both design methods is given.

10 References

[1] EN 14509:2006, Self-supporting double skin metal faced insulating panels –Factory made products –Specifications.

[2] European recommendations for sandwich panels. ECCS/CIB-Report – Publication 257, ECCS TWG 7.9 and CIB W056, 2000.

[3] EN 1993-1-1:2005, Eurocode 3: Design of steel structures – Part 1-1: General rules and rules for buildings

[4]   EN 1991-1-3:2003, Eurocode 1 – Actions on structures – Part 1-3: General actions, Snow loads

[5]   DIN EN 1991-1-3/NA1:2007, National Annex – National determined parameters - Eurocode 1: Actions on structures – Part 1-3: General actions, Snow loads.

[6]   EN 1990:2002: Eurocode – basis of structural design.

[7]   D3.2 - part 3: Test on axially loaded sandwich panels. Deliverable of the EASIE project, September 2010

[8]   D3.2 - part 4: Creeping tests on axially loaded sandwich panels. Deliverable of the EASIE project, September 2010

[9]   Berner, K.: Selbsttragende und aussteifende Sandwichbauteile –Möglichkeiten für kleinere und mittlere Gebäude. Stahlbau 78/2009, S. 298-307

[10] Davies, J.M.: Axially loaded sandwich panels. Journal of Structural Engineering, 133/11, 2212-2230, 1987.

[11] Izabel, D.: Formulaire de Résistance des Matériaux. Tome 4: Détermination des charges critiques de flambement d´éléments comprimés. Les Cahiers Pratiques du SNPPA, 2007.

[12] Plantema, F.J.: Sandwich Construction, The Bending and Buckling of Sandwich Beams, Plates and Shells. New York: Wiley, 1966.

[13] Schulz, U.: Untersuchungen zum Knittern von Sandwichelementen mit ebenen und gesickten Deckschichten. Stahlbau 70/2001, S. 453-463.

[14] Stamm, K., Witte, H.: Sandwichkonstruktionen – Berechnung, Fertigung, Ausführung. Springer – Verlag, 1974.

[15] Taras, A., Greiner, R.: Development of consistent buckling curves for torsional and lateral-torsional buckling. Steel Construction 1 (2008), S. 42-50.

[16] Wadee, M.A.: Experimental Evaluation of Interactive Buckle Localization in Compression Sandwich Panels. Journal of Sandwich Structures and Materials 1999; 1; S. 230-254.

[17] Wadee, M.A.: Effects of periodic and localized imperfections on struts on nonlinear foundations and compression sandwich panels. International Journal of Solids and Structures 37 (2000), S. 1191-1209.

[18] Wölfel, E.: Nachgiebiger Verbund – Eine Näherungslösung und deren Anwendungsmöglichkeiten. Stahlbau 6/1987, S. 173-180.

Design according to 2nd order theory

1 Properties of the sandwich panel

Geometry and material properties of the sandwich can be found on the CE-mark or in approvals:

thickness of the external face sheet	t_{F1}
thickness of the internal face sheet	t_{F2}
thickness of panel	D
width of panel	B
wrinkling stress of the external face sheet	$\sigma_{w,F1}$
wrinkling stress of the internal face sheet	$\sigma_{w,F2}$
yield strength of face sheet	$f_{y,F}$
shear strength of core material	f_{Cv}
shear modulus of core material	G_C
elastic modulus of the faces	E_F
creep coefficient t = 2000h (snow loads)	φ_{2000}
creep coefficient t = 100000h (dead weight loads)	$\varphi_{100.000}$

cross sectional area of face	$A_F = B \cdot t_F$
cross sectional area of core	$A_C = B \cdot D$
bending stiffness	$B_S = E_F \cdot \dfrac{A_{F1} \cdot A_{F2}}{A_{F1} + A_{F2}} \cdot D^2$
shear stiffness	$GA = G_C \cdot A_C$

2 Actions and loads

- Axial loads introduced from ceiling panel:

  N_G dead weight load

  N_S snow load

- If axial loads are introduced in one face sheet only, additional end moments act:

$$M = N \cdot \frac{D}{2}$$

  M^N_G moment caused by N_G

  M^N_S moment caused by N_S

- Transverse loads

  w wind load

- Imperfection:

  e_0 initial deflection

  Initial deflections are considered by equivalent line loads:

  $$q_{e0} = N \cdot 8 \cdot \frac{e_0}{L^2}$$

  $q_{e0,G}$ equivalent line load due to self-weight (N_G)

  $q_{e0,S}$ equivalent line load due to snow (N_S)

- Temperature difference between internal and external face

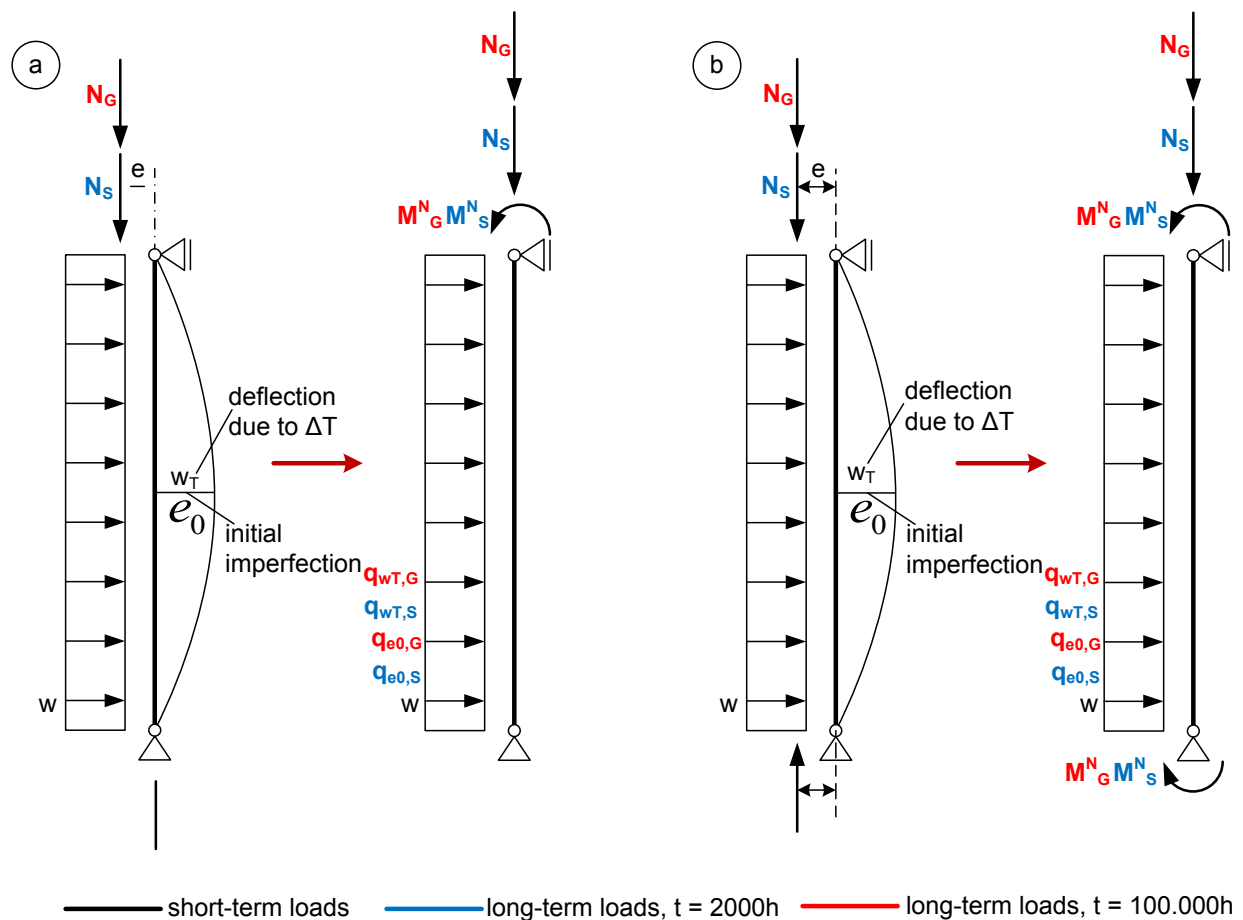 Temperature differences ΔT cause a deflection w_T

  $$w_T = \Delta T \cdot \frac{\alpha_F \cdot L^2}{D \cdot 8}$$

  The deflections w_T is considered by equivalent line loads:

  $$q_{WT} = N \cdot 8 \cdot \frac{w_T}{L^2} = N \cdot \Delta T \cdot \frac{\alpha_F}{D}$$

  $q_{wT,G}$ equivalent line load due to self-weight (N_G)

  $q_{wT,S}$ equivalent line load due to snow (N_S)

| ──── short-term loads | ──── long-term loads, t = 2000h | ──── long-term loads, t = 100.000h |

To determine stress resultants and deflections design loads have to be used (index d). For this purpose load factors γ_F and combination coefficients ψ have to be considered. They are given in EN 14509 or in national standards (e.g. EN 1990 with corresponding national annex).

3   Deflection

Deflections according to 1st order theory, without creep effects:

- Deflection w_W due to wind load

$$w_W^I = w_{W,b}^I(w) + w_{W,v}^I(w)$$

- Deflections w_S due to snow load

$$w_S^I = w_{S,b}^I(q_{e0,S}) + w_{S,b}^I(M_S^N) + w_{S,b}^I(q_{wT,S}) + w_{S,v}^I(q_{e0,S}) + w_{S,v}^I(M_S^N) + w_{S,v}^I(q_{wT,S})$$

- Deflection w_G due to self-weight load

$$w_G^I = w_{G,b}^I(q_{e0,G}) + w_{G,b}^I(M_G^N) + w_{G,b}^I(q_{wT,G}) + w_{G,v}^I(q_{e0,G}) + w_{G,v}^I(M_G^N) + w_{G,v}^I(q_{wT,G})$$

Amplification factor (2nd order theory):

$$\alpha = \frac{1}{1 - \dfrac{N}{N_{cr}}}$$

$$N_{cr} = \frac{N_{ki}}{1 + \dfrac{N_{ki}}{GA}}$$

$$N_{ki} = \pi^2 \cdot \frac{B_S}{s_k^2}$$

$$GA = G_C \cdot A_C$$

Deflection w_t^{II} determined with consideration of creeping and 2nd order theory:

$$w_t^{II} = \left(w_{W,b}^I + w_{W,v}^I + w_{S,b}^I + w_{S,v}^I \cdot (1 + \varphi_{2000}) + w_{G,b}^I + w_{G,v}^I \cdot (1 + \varphi_{100.000}) \right) \cdot \alpha$$

4   Stress resultants

Moments according to 1st order theory, without creep effects:

(See also the following figure)

- Moments M_W due to wind load

$$M_W^I = M_W^I(w)$$

- Moments M_S due to snow loads:

$$M_S^I = M_S^I(q_{e0,S}) + M_S^I(M_S^N) + M_S^I(q_{wT,S})$$

- Moments M_G due to self-weight load:

$$M_G^I = M_G^I(q_{e0,G}) + M_G^I(M_G^N) + M_G^I(q_{wT,G})$$

Transverse force according to 1st order theory, without creep effects:

Transverse force according to 1st order theory, without creep effects:

(See also the following figure)
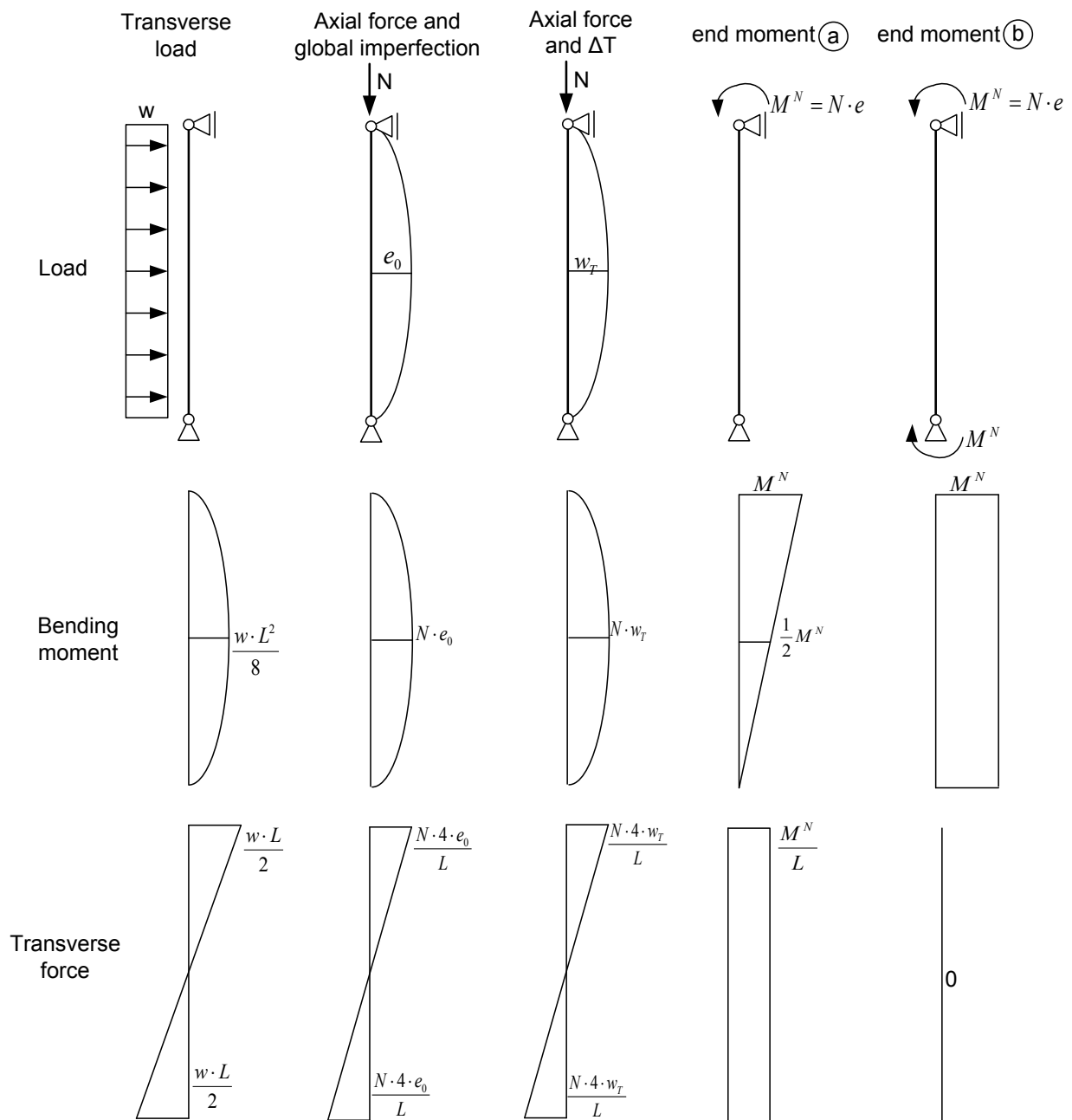
- Transverse force V_W due to wind load

$$V_W^I = V_W^I(w)$$

- Transverse force V_S due to snow loads:

$$V_S^I = V_S^I(q_{e0,S}) + V_S^I(M_S^N) + V_S^I(q_{wT,S})$$

- Transverse force V_G due to self-weight load:

$$V_G^I = V_G^I(q_{e0,G}) + V_G^I(M_G^N) + V_G^I(q_{wT,G})$$

Coefficient for consideration of creep effects:

$$\varphi_{St} = \frac{k}{1+k} \cdot \varphi_t$$

$$k = \frac{w_{lt,v}}{w_{lt,b}} = \frac{B_S}{GA} \cdot \frac{\int V\overline{V}dx}{\int M\overline{M}dx}$$

Factor k for typical loads on wall panels (without temperature difference):

a)

$$k = \frac{B_S}{GA \cdot L^2} \cdot \frac{48 \cdot e_0}{3 \cdot e + 5 \cdot e_0}$$

b)

$$k = \frac{B_S}{GA \cdot L^2} \cdot \frac{48 \cdot e_0}{6 \cdot e + 5 \cdot e_0}$$

Stress resultants determined with consideration of creeping and 2nd order theory

- Moment:

$$M_t^{II} = \left(M_W^I + M_S^I \cdot (1 + \varphi_{S2000}) + M_G^I \cdot (1 + \varphi_{S100.000})\right) \cdot \alpha$$

- Transverse force:

$$V_t^{II} = \left(V_W^I + V_S^I \cdot (1 + \varphi_{S2000}) + V_G^I \cdot (1 + \varphi_{S100.000})\right) \cdot \alpha$$

- Normal force:

$$N = N_S + N_G$$

5   Stresses in face sheets and core

- Normal stress in compressed face sheet:

$$\sigma_F = \frac{M_t^{II}}{D \cdot A_{F1}} + \frac{N}{A_{F1} + A_{F2}}$$

- Normal stress in face sheet subjected to tension:

$$\sigma_F = \frac{M_t^{II}}{D \cdot A_{F2}} - \frac{N}{A_{F1} + A_{F2}}$$

- Shear stress in the core material:

$$\tau_C = \frac{V_t^{II}}{A_C}$$

6   Limitation of deflection (serviceability limit state)

$$w_t \leq w_{\max}$$

For wall panels according to EN 14509:

$$w_{\max} = \frac{L}{100}$$

7   Limitation of stresses (ultimate limit state)

- Compression stress in face sheets:

$$\sigma_{F,d} \leq \frac{\sigma_{w,k}}{\gamma_M}$$

- Tensile stress in face sheet

$$\sigma_{F,d} \leq \frac{f_{yF,k}}{\gamma_M}$$

- Shear stress in core material:

$$\tau_{C,d} = \frac{f_{Cv,k}}{\gamma_M}$$

Design according to equivalent member method

1   Panels loaded only by axial load N

$$\frac{N_{Ed}}{\chi \cdot N_{Rd}} \le 1,0$$

$$N_{Rd} = \frac{N_w}{\gamma_M} = \frac{\sigma_w \cdot (A_{F1} + A_{F2})}{\gamma_M}$$

$$\sigma_w = 0,5 \cdot \sqrt{E_F.E_C.G_C} \quad \text{or alternatively determined by testing}$$

$$\chi = \frac{1}{\phi + \sqrt{\phi^2 - \lambda^2}}$$

$$\phi = 0,5 \cdot \left(1 + \alpha \cdot \sqrt{\lambda^2 - \lambda_{GA}^2} + \lambda^2\right)$$

$$\lambda_{GA} = \sqrt{\frac{N_W}{GA}}$$

$$\lambda_{ki} = \sqrt{\frac{N_w}{N_{crit}}}$$

$$N_{crit} = \frac{\pi^2 B_s}{L^2}$$

$$\lambda = \sqrt{\lambda_{ki}^2 + \lambda_{GA}^2}$$

$$\alpha = \frac{2 \cdot \overline{e}_0}{D} \cdot \pi \cdot \sqrt{\frac{B_S}{N_w}}$$

$$\overline{e}_0 = \frac{e_0}{L}$$

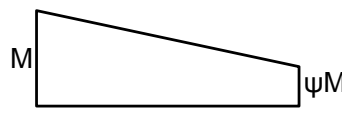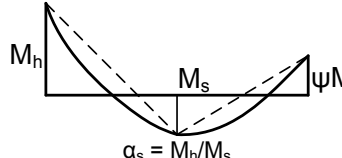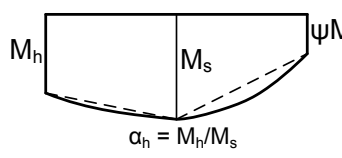## 2   Panels loaded by axial load N and bending moment M

$$\frac{N_{Ed}}{\chi \cdot N_{Rd}} + k_{yy} \frac{M_{Ed}}{M_{Rd}} \le 1$$

N_{Rd}, χ according to the formulae given in section 1

$$M_{Rd} = \frac{M_w}{\gamma_M} = \frac{D \cdot A_F \cdot \sigma_w}{\gamma_M}$$

$$k_{yy} = C_{my} \cdot (1 + 0,8 \cdot \frac{N}{\chi \cdot N_w})$$

C_{my}: equivalent uniform moment factor according to EN 1993-1-1, table B.3

moment distribution			C_{my}	
			uniformly distributed load	point load
M ⎥‾‾‾‾⎤ ⎥ψM	$-1 \leq \psi \leq 1$		$0,6 + 0,4\psi \geq 0,4$	
M_h M_s ψM_h $\alpha_s = M_h/M_s$	$0 \leq \alpha_s \leq 1$	$-1 \leq \psi \leq 1$	$0,2 + 0,8\alpha_s \geq 0,4$	$0,2 + 0,8\alpha_s \geq 0,4$
	$-1 \leq \alpha_s < 0$	$0 \leq \psi \leq 1$	$0,1 - 0,8\alpha_s \geq 0,4$	$-0,8\alpha_s \geq 0,4$
		$-1 \leq \psi < 0$	$0,1(1-\psi) - 0,8\alpha_s \geq 0,4$	$0,2(-\psi) - 0,8\alpha_s \geq 0,4$
M_h M_s ψM_h $\alpha_h = M_h/M_s$	$0 \leq \alpha_h \leq 1$	$-1 \leq \psi \leq 1$	$0,95 + 0,05\alpha_h$	$0,90 + 0,10\alpha_h$
	$-1 \leq \alpha_h < 0$	$0 \leq \psi \leq 1$	$0,95 + 0,05\alpha_h$	$0,90 + 0,10\alpha_h$
		$-1 \leq \psi < 0$	$0,95 + 0,05\alpha_h(1+2\psi)$	$0,90 - 0,10\alpha_h(1+2\psi)$